

# Use of Third-party Aircraft Performance Tools in the Development of the Aviation Environmental Design Tool (AEDT)

---

Prepared for:

U.S. Department of Transportation  
Federal Aviation Administration  
Office of Environment and Energy (AEE)  
Washington, DC 20591

Prepared by:

U.S. Department of Transportation  
Research and Innovative Technology Administration  
John A. Volpe National Transportation Systems Center  
Environmental and Energy Systems  
Cambridge, MA 02142

Volpe Report number: DOT-VNTSC-FAA-11-08

July, 2011

## NOTICE

This document is disseminated under the sponsorship of the Department of Transportation in the interest of information exchange. The United States Government assumes no liability for its contents or use thereof. This report does not constitute a standard, specification, or regulation.

The United States Government does not endorse products or manufacturers. Trade or manufacturers' names appear herein solely because they are considered essential to the object of this document.

# REPORT DOCUMENTATION PAGE

Form Approved  
OMB No. 0704-0188

Public reporting burden for this collection of information is estimated to average 1 hour per response, including the time for reviewing instructions, searching existing data sources, gathering and maintaining the data needed, and completing and reviewing the collection of information. Send comments regarding this burden estimate or any other aspect of this collection of information, including suggestions for reducing this burden, to Washington Headquarters Services, Directorate for Information Operations and Reports, 1215 Jefferson Davis Highway, Suite 1204, Arlington, VA 22202-4302, and to the Office of Management and Budget, Paperwork Reduction Project (0704-0188), Washington, DC 20503.

|  |  |   |   |  |
|--|--|---|---|--|
| 1. AGENCY USE ONLY (Leave blank)   |  | 2. REPORT DATE<br>July 2011                             | 3. REPORT TYPE AND DATES COVERED<br>Final Report<br>August 2010 to July 2011                                  |  |
| 4. TITLE AND SUBTITLE<br><br>Use of Third-party Aircraft Performance Tools in the Development of the Aviation Environmental Design Tool (AEDT)   |  |   | 5. FUNDING NUMBERS<br><br>FA4TA3/JT195  |  |
| 6. AUTHOR(S)<br><br>Joeri Dons <sup>(1)</sup> , Jan Mariens <sup>(1)</sup> , Gregory D. O'Callaghan <sup>(1)</sup>   |  |   | 8. PERFORMING ORGANIZATION REPORT NUMBER<br><br>DOT-VNTSC-FAA-11-08   |  |
| 7. PERFORMING ORGANIZATION NAME(S) AND ADDRESS(ES)<br>U.S. Department of Transportation<br>Research and Innovative Technology Administration<br>John A. Volpe National Transportation Systems Center<br>Environmental Measurement and Modeling Division, RVT-41<br>Cambridge, MA 02142   |  |   | 10. SPONSORING/MONITORING AGENCY REPORT NUMBER  |  |
| 9. SPONSORING/MONITORING AGENCY NAME(S) AND ADDRESS(ES)<br><br>U.S. Department of Transportation<br>Federal Aviation Administration<br>Office of Environment and Planning<br>Washington, DC 20591  |  |   | 11. SUPPLEMENTARY NOTES<br>(1) International Intern, STC, Hampton, VA 23666<br>Delft University of Technology |  |
| 12a. DISTRIBUTION/AVAILABILITY STATEMENT<br>This document is available to the public through the National Technical Information Service, Springfield, VA 22161   |  |   | 12b. DISTRIBUTION CODE  |  |
| 13. ABSTRACT (Maximum 200 words)<br><br>This report documents work done to enhance terminal area aircraft performance modeling in the Federal Aviation Administration's Aviation Environmental Design Tool. A commercially available aircraft performance software tool was used to develop data in a form usable by the Aviation Environmental Design Tool. These data were compared to actual aircraft performance data measured by flight data recorder systems. The terminal area fuel consumption data was shown to average about 2% different from the measured fuel consumption for departures and about 5% different for arrivals. |  |   |   |  |
| 14. SUBJECT TERMS<br>Aviation fuel consumption, Federal Aviation Administration  |  |   | 15. NUMBER OF PAGES<br>60   |  |
|  |  |   | 16. PRICE CODE  |  |
| 17. SECURITY CLASSIFICATION OF REPORT<br>Unclassified  | 18. SECURITY CLASSIFICATION OF THIS PAGE<br>Unclassified | 19. SECURITY CLASSIFICATION OF ABSTRACT<br>Unclassified | 20. LIMITATION OF ABSTRACT<br><br>Unlimited   |  |

NSN 7540-01-280-5500

Standard Form 298 (Rev. 2-89)  
Prescribed by ANSI Std. Z39-18 298-102



# Use of Third-party Aircraft Performance Tools in the Development of the Aviation Environmental Design Tool (AEDT) \*

DISSERTATION

SUBMITTED IN PARTIAL FULFILLMENT OF THE REQUIREMENTS FOR THE  
DEGREE OF MASTER OF SCIENCE IN AEROSPACE ENGINEERING  
DELFT UNIVERSITY OF TECHNOLOGY, THE NETHERLANDS

AUGUST 2010 – DECEMBER 2010

AUTHORS:

JOERI DONS  
INTERNATIONAL INTERN, STC HAMPTON VA  
DELFT UNIVERSITY OF TECHNOLOGY

JAN MARIENS  
INTERNATIONAL INTERN, STC HAMPTON VA  
DELFT UNIVERSITY OF TECHNOLOGY

GREGORY D. O'CALLAGHAN  
INTERNATIONAL INTERN, STC HAMPTON VA  
DELFT UNIVERSITY OF TECHNOLOGY

PROJECT SUPERVISOR:

DAVID A. SENZIG  
USDOT/VNTSC

ACADEMIC ADVISOR:

DR. AMAR CHOUDRY  
STC HAMPTON VA

\* SUPPORTED BY USDOT CONTRACT# DTRT57-10-P-80006/01027



# Preface

Although air travel is one of the safest modes of transportation, the use of airplanes has some downsides as well. One the major downsides is the contribution to global greenhouse gas emissions. Civil aviation contributes about two percent of CO<sub>2</sub> and three percent of NO<sub>x</sub> emissions. For several years both governments and aviation organizations, e.g. FAA or ICAO, have set limits and quotas on the amount of emissions. Penalties are given to airlines which for instance exceed the limit of CO<sub>2</sub> emission. The limits and quotas are based on fuel consumption analysis since this is the main driver for emissions. Improvement in fuel consumption modeling is important as policy makers seek to improve the efficiency of the national and international airspace system while considering the associated environmental impacts.

The U.S. Federal Aviation Administration (FAA) is in the process of transitioning from its legacy environmental tools to a single integrated tool: Aviation Environmental Design Tool (AEDT). This new tool supports a higher level of fidelity in fuel consumption modeling in the terminal area, but the tool is however still in process. One part of this process is explained in this report. The report examines the use of third-party aircraft performance tools, i.e. Project Interactive Analysis and Optimization (PIANO) tool, in the development of the Aviation Environmental Design Tool. PIANO is used to extract aerodynamic and performance data for aircraft manufactures that did not provide neither of this data.

This report is developed for U.S. Department of Transportations Volpe National Systems in Cambridge, Massachusetts and for Science and Technology Corporation in Hampton, Virginia. It is also submitted in partial fulfillment of the requirements for the degree of Master of Science in Aerospace Engineering Delft University of Technology, The Netherlands.

This report is the concluding part of the internship of three international interns from the Delft University of Technology at the Volpe National Systems Center, a subdivision of U.S. Department of Transportations. Joeri Dons is a master student with the Systems Engineering and Aircraft Design Department at the Faculty of Aerospace Engineering at the Delft University of Technology. He a holds a Bachelor of Science in aerospace engineering from the Delft University of Technology. Jan Mariens is a master student with the Systems Engineering and Aircraft Design Department at the Faculty of Aerospace Engineering at the Delft University of Technology. He a holds a Bachelor of Science in aerospace engineering from the Delft University of Technology. Gregory D. O’Callaghan is a master student with the Air Transport and Operations Department at the Faculty of Aerospace Engineering at the Delft University of Technology.

First of all, we would like to thank David A. Senzig, our project supervisor, for his expertise

and excellent guidance during our internship. David is an engineer with the U.S. Department of Transportation Volpe Center's Environmental and Energy Systems Center of Innovation in Cambridge, Massachusetts. We would also like to thank Dr. A. Choudry, our academic advisor, for making this internship possible and for his continuous support and feedback.

Our thanks go out to George J. Noel who assisted when David was unavailable. George is an engineer with the U.S Department of Transportation Volpe Center's Air Quality Facility in Cambridge, Massachusetts. This work was funded by the FAA's Office of Environment and Energy. We also thank Ralph Iovinelle, Program Manager for AEDT, for supporting this work.

Finally, we would like to thank our families and friends for their support given during our stay in the United States of America.

Joeri Dons  
Jan Mariens  
Gregory D. O'Callaghan

November 16, 2010  
Cambridge, Massachusetts  
The United States of America

# Summary

The FAA has recently updated the airport terminal area fuel consumption methods used in the Aviation Environmental Design Tool (AEDT). These updates are based on fitting data from a commercial third party aircraft performance program (PIANO – Project Interactive Analysis and Optimization) to previously developed empirical equations. These algorithm updates have adequate fidelity in the terminal area to assist air transportation policy makers in weighing the costs and benefits of competing environmental and economic demands. Comparison with Flight Data Recorder (FDR) information for in-service airline operations shows that the combination of new aircraft data with the methods of the FAA’s models can accurately capture the fuel consumption consequences of different terminal departure and arrival procedures within a reasonable level of uncertainty.

This report presents the use of the software tool PIANO to develop a new source of aircraft performance and fuel consumption data for computing terminal area airplane fuel consumption that has been implemented in FAA’s AEDT. The terminal area covers the departures and arrivals of flights till 10,000 feet above ground level. The data is developed using PIANO and applied in the AEDT algorithms to improve, with respect to the BADA 3.8 (EUROCONTROL’s Base of Aircraft Data – old method), the fuel consumption modeling in the terminal area.

There are three types of coefficients used in the AEDT’s algorithms for fuel consumption modeling, i.e. TSFC (Thrust Specific Fuel Consumption), thrust and aerodynamics coefficients.

For the Airbus A320 family of aircraft during departures, the prior methods differed by about 10 to 15% by measured values, while the new method only differs by 0 to 5%. For this family of aircraft, this modeling improvement is on the order of 100 lb of fuel per departure. The improvements for the Airbus A330/A340 family with the new method during departures, show differences within 5% of the measured fuel consumption. The results show that the generated departure aerodynamic and thrust coefficient sets show sufficient fidelity to simulate departures in AEDT and that the generated TSFC coefficients are reliable to model fuel consumption.

The fuel consumption for arrival operations also shows improvements, though not as significant as with the departures. For the limited number of arrivals that were analyzed, the average difference from the measured fuel consumption decreased from about 9% (BADA 3.8) to 5%. The 4% improvement indicates that the generated aerodynamic coefficients are sufficiently reliable to simulate an arrival and that the generated TSFC coefficients are accurate enough to model the fuel consumption. However, due to the limited number of validation results it is not possible to make the improvement statement conclusive. This requires more validation results.

These new coefficients will allow more accurate modeling for aircraft fuel consumption in the terminal area. This will provide the FAA with two benefits. First, with these new coefficients AEDT will now calculate more accurate aircraft fuel consumption which will allow more accurate prediction of the environmental impacts of aviation. Second, use of AEDT in planning processes (such as airspace redesigns) will lead to better environmental decision-making.





# Contents

|   |           |
|---|-----------|
| Preface   | i         |
| Summary   | iii       |
| List of Figures   | vii       |
| List of Tables  | ix        |
| Nomenclature  | xi        |
| <b>1 Introduction</b>   | <b>1</b>  |
| <b>I Determination of Departure and Arrival Coefficients</b>        | <b>3</b>  |
| <b>2 Departure TSFC and Thrust Coefficients</b>                     | <b>5</b>  |
| 2.1 Departure TSFC and thrust equations . . . . .                   | 5         |
| 2.1.1 Departure TSFC equation . . . . .                             | 5         |
| 2.1.2 Thrust equation . . . . .                                     | 6         |
| 2.2 Data generation using PIANO . . . . .                           | 6         |
| 2.3 Generating TSFC/Thrust coefficients from data set . . . . .     | 7         |
| 2.3.1 Thrust coefficients determination . . . . .                   | 9         |
| 2.3.2 Departure TSFC coefficients determination . . . . .           | 9         |
| <b>3 Departure Aerodynamic Coefficients</b>                         | <b>11</b> |
| 3.1 Departure aerodynamic equations . . . . .                       | 11        |
| 3.1.1 Initial-climb calibrated airspeed coefficient $C_f$ . . . . . | 11        |
| 3.1.2 Takeoff ground-roll coefficient $B_f$ . . . . .               | 12        |
| 3.1.3 Departure drag-over-lift coefficient $R_f$ . . . . .          | 12        |
| 3.2 Data generation using PIANO . . . . .                           | 13        |
| 3.2.1 FDR based departure profiles . . . . .                        | 14        |
| 3.2.2 NOT-FDR based departure profiles . . . . .                    | 15        |
| 3.3 Data processing of PIANO output . . . . .                       | 16        |
| <b>4 Arrival TSFC Coefficients</b>                                  | <b>19</b> |
| 4.1 Arrival TSFC equation . . . . .                                 | 19        |
| 4.2 Data generation using PIANO . . . . .                           | 19        |
| 4.3 Generating arrival TSFC coefficients from data set . . . . .    | 20        |

---

|           |  |           |
|-----------|--|-----------|
| <b>5</b>  | <b>Arrival Aerodynamic Coefficients</b>  | <b>23</b> |
| 5.1       | Arrival aerodynamic equations . . . . .  | 23        |
| 5.1.1     | Arrival drag over lift coefficient $R_f$ . . . . .                             | 23        |
| 5.1.2     | Landing speed coefficient . . . . .  | 24        |
| 5.2       | Data generation using PIANO and data processing . . . . .                      | 24        |
| <b>II</b> | <b>Validation of PIANO Data with FDR Information</b>                           | <b>27</b> |
| <b>6</b>  | <b>Departure Operations</b>  | <b>29</b> |
| 6.1       | Validation of aircraft with manufacturer provided aerodynamic coefficients . . | 29        |
| 6.1.1     | Validation of A319-100 . . . . .   | 30        |
| 6.1.2     | A320-200 validation . . . . .  | 32        |
| 6.1.3     | A321-200 validation . . . . .  | 33        |
| 6.2       | Validation of airplanes with PIANO generated aerodynamic coefficients . . .    | 34        |
| 6.2.1     | A330-200 validation . . . . .  | 35        |
| 6.2.2     | A340-300 validation . . . . .  | 35        |
| 6.2.3     | A340-500 validation . . . . .  | 36        |
| 6.3       | Conclusions of the departure validation . . . . .                              | 37        |
| <b>7</b>  | <b>Arrival Operations</b>  | <b>39</b> |
| 7.1       | Validation of arrival TSFC and aerodynamic coefficients . . . . .              | 39        |
| 7.1.1     | Example of replicating an FDR flight in AEDT . . . . .                         | 40        |
| 7.1.2     | Summary of results . . . . .   | 41        |
| 7.2       | Conclusion of the arrival validation . . . . .                                 | 42        |
| <b>8</b>  | <b>Conclusions and Recommendations</b>   | <b>43</b> |
| 8.1       | Conclusions . . . . .  | 43        |
| 8.2       | Recommendations . . . . .  | 44        |
|           | <b>Bibliography</b>  | <b>47</b> |
|           | <b>Appendices</b>  |           |
| <b>A</b>  | <b>Thrust Coefficients</b>   | <b>49</b> |
| <b>B</b>  | <b>TSFC Coefficients</b>   | <b>51</b> |
| <b>C</b>  | <b>Aerodynamic Coefficients</b>  | <b>55</b> |
| <b>D</b>  | <b>AEDT Output Example</b>   | <b>59</b> |

# List of Figures

|     |  |    |
|-----|--|----|
| 2.1 | Example of the point performance function in PIANO [8] showing the input entries . . . . .           | 7  |
| 2.2 | Departure data collection region . . . . .   | 8  |
| 3.1 | Example of the flight maneuver function in PIANO [8] showing the input entries                       | 13 |
| 3.2 | CAS (left) and flap angle (right) of FDR data from an A340-500 departure .                           | 15 |
| 3.3 | Output example of flight maneuver in PIANO . . . . .   | 17 |
| 4.1 | Arrival data collection region . . . . .   | 20 |
| 4.2 | TSFC loops (Engine characteristics, PIANO [8]) . . . . .   | 21 |
| 5.1 | The Final Approach maneuver function in PIANO [8] . . . . .  | 24 |
| 6.1 | A319-100 validation for initial climb to 10,000 ft AGL, no extra TOW . . . .                         | 30 |
| 6.2 | A319-100 validation for initial climb to 10,000 ft AGL, with extra TOW at 110,000 lb . . . . .       | 31 |
| 6.3 | Curve fit result for the A319-100, initial climb to 10,000ft AGL, extra TOW at 110,000 lb . . . . .  | 32 |
| 6.4 | Curve fit result for the A320-200, initial climb to 10,000 ft AGL, extra TOW at 125,000 lb . . . . . | 33 |
| 6.5 | Curve fit result for the A321-200, initial climb to 10,000 ft AGL, extra TOW at 130,000 lb . . . . . | 34 |
| 6.6 | Curve fit result for the A330-200, initial climb to 10,000 f t AGL, extra TOW 310,000 lb . . . . .   | 35 |
| 6.7 | Curve fit result for the A340-300, initial climb to 3000 ft AGL, without extra TOW . . . . .         | 36 |
| 6.8 | Curve fit result for the A340-500, initial climb to 10,000 ft AGL, extra TOW at 450,000 lb . . . . . | 37 |
| 7.1 | Output AEDT simulation of the A319-100 . . . . .   | 41 |
|     | (a) Approach profile . . . . .   | 41 |
|     | (b) True airspeed . . . . .  | 41 |
| 7.2 | Output AEDT simulation of the A319-100 . . . . .   | 41 |
|     | (a) Fuel flow . . . . .  | 41 |
|     | (b) Consumed fuel . . . . .  | 41 |



# List of Tables

|     |   |    |
|-----|---|----|
| 2.1 | Point performance function (PIANO) inputs for departure operations . . . .                      | 7  |
| 3.1 | Departure template of the Airbus A330-200 . . . . .   | 14 |
| 3.2 | Departure template of the Airbus A340-300 . . . . .   | 14 |
| 3.3 | Departure template of the Airbus A340-500 . . . . .   | 15 |
| 3.4 | General departure template . . . . .  | 16 |
| 3.5 | Departure template of the ATR 42-500 and ATR 72-500 . . . . .                                   | 16 |
| 3.6 | Departure template of the Fokker F70 . . . . .  | 16 |
| 4.1 | Point performance function (Piano) inputs for arrival operations . . . . .                      | 20 |
| 5.1 | Example of calculated coefficients for flap/landing gear combinations of the A318-100 . . . . . | 25 |
| 6.1 | Average error of A319-100 validation . . . . .  | 32 |
| 6.2 | Average error of A320-200 validation . . . . .  | 33 |
| 6.3 | Average error of A321-200 validation . . . . .  | 33 |
| 6.4 | Average error of A330-200 validation . . . . .  | 35 |
| 6.5 | Average error of A340-300 validation . . . . .  | 36 |
| 6.6 | Average error of A340-500 validation . . . . .  | 37 |
| 6.7 | Departure validation summary . . . . .  | 38 |
| 7.1 | Procedural profile to replicate FDR arrival . . . . .   | 40 |
| 7.2 | Model comparison results . . . . .  | 42 |



# Nomenclature

## Abbreviations

|       |   |
|-------|---|
| AAE   | Average Absolute Error                        |
| AEDT  | Aviation Environmental Design Tool            |
| AFE   | Above Field Elevation                         |
| AGL   | Above Ground Level                            |
| ATM   | Air Traffic Management                        |
| BADA  | Base of Aircraft Data                         |
| BCOP  | Boeing Climb-out Program                      |
| CAS   | Calibrated Airspeed                           |
| FAA   | Federal Aviation Administration               |
| FDR   | Flight Data Recorder                          |
| ISA   | International Standard Atmosphere             |
| LSZH  | Zurich Airport                                |
| MSL   | Mean Sea Level                                |
| MTOW  | Maximum Takeoff Weight                        |
| NLW   | Normal Landing Weight                         |
| OMAA  | Abu Dhabi International Airport               |
| PIANO | Project Interactive Analysis and Optimization |
| TAS   | True Airspeed                                 |
| TOFL  | Takeoff Field Length                          |
| TOW   | Takeoff Weight                                |
| TSFC  | Thrust Specific Fuel Consumption              |



## Notations

|                      |  |                      |
|----------------------|--|----------------------|
| $C_f$                | Initial-climb calibrated airspeed coefficient    | [-]                  |
| $B_f$                | Takeoff ground-roll coefficient                  | [-]                  |
| $D_f$                | Landing speed coefficient                        | [-]                  |
| $F_0$                | Maximum thrust at sea level static conditions    | [lbf]                |
| $\frac{F_N}{\delta}$ | Corrected net thrust                             | [lbf]                |
| $h$                  | Altitude   | [ft]                 |
| $\dot{m}_f$          | Fuel flow  | [lbs/hr]             |
| $M$                  | Mach Number                                      | [-]                  |
| $N$                  | Number of engines supplying thrust               | [-]                  |
| $P$                  | Pressure   | [N/m <sup>2</sup> ]  |
| $P_0$                | ISA pressure at sea level                        | [N/m <sup>2</sup> ]  |
| $R_f$                | Drag-over-lift ratio coefficient                 | [-]                  |
| $S_g$                | Ground-roll distance                             | [ft]                 |
| $T_0$                | ISA temperature at sea level                     | [Kelvin]             |
| TSFC                 | Thrust specific fuel consumption                 | [lb/hr/lbf]          |
| $v_2$                | Takeoff safety speed                             | [knots]              |
| $v_i$                | Calibrated airspeed at initial climb (35 ft AGL) | [knots]              |
| $V$                  | Calibrated airspeed                              | [knots]              |
| $W$                  | Aircraft weight                                  | [lb]                 |
| $\delta$             | Pressure ratio                                   | [-]                  |
| $\gamma$             | Flight path angle                                | [deg]                |
| $\lambda$            | Temperature lapse rate                           | [Kelvin/m]           |
| $\theta$             | Temperature ratio                                | [-]                  |
| $\rho$               | Density  | [kg/m <sup>3</sup> ] |
| $\rho_0$             | ISA density at sea level                         | [kg/m <sup>3</sup> ] |

# Chapter 1

## Introduction

The U.S. Federal Aviation Administration (FAA) is in the process of transitioning from its legacy environmental tools to a single integrated tool. This new tool is the Aviation Environmental Design Tool (AEDT), a next generation suite of integrated aviation environmental tools [9] [4]. AEDT will provide users with the ability to assess the interdependencies between aviation-produced noise, fuel consumption and emissions.

For fuel consumption analyses (upon which emission analyses depend), development versions of AEDT have relied on data from EUROCONTROL's Base of Aircraft Data (BADA) [2]. The BADA fuel consumption model uses an energy-balance thrust model and Thrust Specific Fuel Consumption (TSFC) modeled as a function of airspeed. BADA information on airplane performance and fuel consumption exists for a large part of the civil fleet. The BADA fuel consumption model has been shown to work well in cruise, with differences from airline reported fuel consumption of about 3% [6, 10]. However, comparisons of BADA-predicted and actual airline fuel consumption (reported via their FDR system) in the terminal area revealed that BADA does not perform as accurately in this region compared with cruise.

To support a higher level of modeling fidelity in the terminal area, the FAA initiated a program to work with the manufacturers to use their performance tools to improve fuel consumption modeling in this region. As a result of this effort, the Boeing Company provided their low speed performance model to the FAA; this model was used to improve the terminal area for the Boeing aircraft in the fleet [14].

To provide information on the other manufacturers aircraft, the FAA purchased the Project Interactive Analysis and Optimization (PIANO) tool, developed by Lissys [8]. In other words, PIANO is used as third-party aircraft performance tool in the development of the database of AEDT.

The objective of this report is to inform the reader how low speed aircraft performance algorithms and methodologies are improved, by using PIANO, within the terminal airspace to increase AEDT modeled accuracy of fuel burn estimates within the terminal area. PIANO contains aerodynamic and performance data for a large number of transport aircraft in the global civil fleet. For those aircraft where manufacturers have already provided aerodynamic data for the FAA's legacy tools, PIANO was used to determine the Thrust Specific Fuel Consumption (TSFC) data. Note that these aerodynamic data are in the form described in [16] and enhanced in [3]. Those aircraft without any data in the legacy tools had both aerodynamic and TSFC data generated using PIANO. For all aircraft, the data developed

was within the domain of the terminal area, i.e. below 10,000 feet above field elevation (AFE) and generally within 16,000 feet mean sea level (MSL). Validation was conducted by comparing in-service airline fuel consumption (Flight Data Recorder information) with modeled fuel consumption data.

This report is divided into two parts. The first part discusses the determination of the departure and arrival coefficients. The determination of the departure TSFC and thrust coefficients is given in chapter 2. Chapter 3 discusses the determination of the departure aerodynamic coefficients. The determination of the arrival TSFC- and aerodynamic coefficients is treated in chapter 4 and 5, respectively. Chapters 2 through 5 have the same structure. First is the theory behind the equations (TSFC, thrust and aerodynamic) explained. Subsequently the extraction method for PIANO is briefly discussed. The last section explains possible data processing steps.

The validation of the new determined coefficients is given in part two of the report. Chapter 6 explains the validation of the departure operations. Aircraft with manufacturer aerodynamic coefficients as well as aircraft with PIANO generated aerodynamic coefficients are validated. The validation of the arrival operations is given in chapter 7. Conclusions and recommendations can be found in the last chapter of this report.

## **Part I**

# **Determination of Departure and Arrival Coefficients**



## Chapter 2

# Departure TSFC and Thrust Coefficients

The departure Thrust Specific Fuel Consumption (TSFC) coefficients and thrust coefficients are one of the fundamentals for the current environmental model and fuel consumption model in AEDT. First the departure TSFC equation and the thrust equation are introduced in section 2.1. Consequently, the methods used to generate aircraft data sets using the software tool PIANO are elaborated in section 2.2. Finally, the aircraft state parameters are derived from the generated aircraft data set. The data processing breakdown is discussed in section 2.3.

### 2.1 Departure TSFC and thrust equations

This section introduces the TSFC and thrust equation as well as the elucidation of their parameters.

#### 2.1.1 Departure TSFC equation

The departure model, based on equation of SAE-AIR-1845 [16], is given below:

$$\frac{\text{TSFC}}{\sqrt{\theta}} = K_1 + K_2 \cdot M + K_3 \cdot h + K_4 \cdot \left( \frac{F_N}{\delta} \right) \quad (2.1)$$

where

|                      |  |
|----------------------|--|
| $M$                  | aircraft Mach number   |
| $h$                  | altitude (ft) above mean sea level (MSL)   |
| $\frac{F_N}{\delta}$ | corrected net thrust per engine (lbf)  |
| $\theta$             | temperature ratio (altitude dependent)   |
| $K_i$                | regression coefficients to be determined for individual airplane types (for $i = 1, 2, 3, 4$ ) |

For each engine/airplane combination, the regression coefficients are determined by:

- Generating data for a wide range of operational conditions (section 2.2)

- Collecting this data into an organized structure
- Statistically analyzing those data (to determine the coefficients, see section 2.3)

### 2.1.2 Thrust equation

An important consideration for a TSFC algorithm (equation 2.2) is the type of thrust model with which it will be used. The thrust model described in [16] and as enhanced in [3], uses a linear relationship on velocity and a quadratic relationship on altitude to predict the thrust in the two departure modes, namely: the takeoff power and the maximum climbing power. The thrust model is prescribed by the following equation.

$$\frac{F_N}{\delta} = E + F \cdot V + G_A \cdot h + G_B \cdot h^2 + H \cdot T_C \quad (2.2)$$

where

|                      |  |
|----------------------|--|
| $V$                  | calibrated airspeed (knots)  |
| $h$                  | altitude (ft) above mean sea level (MSL)   |
| $\frac{F_N}{\delta}$ | corrected net thrust per engine (lbf)  |
| $T_C$                | temperature ( $^{\circ}\text{C}$ ) at the aircraft   |
| $E, F, G_A, G_B, H$  | regression coefficients that depend on power state (max-takeoff or max-climb power) and temperature state (below or above engine breakpoint temperature) |

The engine is operating in a region where temperature effects do not matter – this is below the ‘break-point’ of the engine. The temperature change below this break-point does not affect the engine performance. For this reason the temperature regression coefficient  $H$  can be neglected. As similar to the departure TSFC coefficients determination, the thrust coefficients require filtered data sets (section 2.3) and a multiple regression analysis can be applied here to determine these coefficients. The thrust coefficients are derived for rated takeoff power and maximum climb power, which is part of the filtering process that is explained in the next section.

## 2.2 Data generation using PIANO

The data is generated using the software tool PIANO and its *point performance* function. This function, shown in figure 2.1, requires the following aircraft states as input: the altitude (in ft) and the Mach number (note that the thrust entry is left blank). These inputs match the expected flight regime for the aircraft being modeled. The point performance function gives the following outputs: maximum available thrust, fuel flow and TSFC values for cruise rating, climb rating, continuous rating and takeoff rating for each (data) point. The data generation using this function in PIANO with the flight regimes as inputs, is automated using WINBATCH [18].

The inputs provided for the point performance function are based on FDR data and research on existing departure operations. They are chosen such that they are valid for all planes that need to be processed. The inputs consist of combinations of ranging Mach numbers and aircraft operating altitudes, as shown in table 2.1.

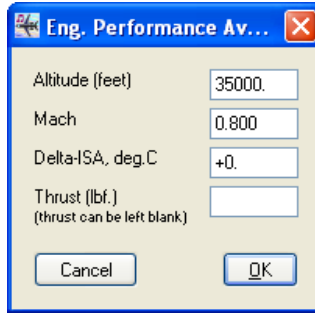


**Figure 2.1:** Example of the point performance function in PIANO [8] showing the input entries

**Table 2.1:** Point performance function (PIANO) inputs for departure operations

|         | Mach number [-]             | Altitude [ft]                  |
|---------|-----------------------------|--------------------------------|
| Block 1 | 0 – 0.36 (steps of 0.12)    | 0 – 2500 (steps of 500)        |
| Block 2 | 0 – 0.46 (steps of 0.12)    | 2500 – 7000 (steps of 500)     |
| Block 3 | 0.25 – 0.46 (steps of 0.07) | 7000 – 10,000 (steps of 500)   |
| Block 4 | 0.4 – 0.6 (steps of 0.04)   | 10,000 – 16,000 (steps of 500) |

The green crosshatched blocks in figure 2.2 show the expected flight regime for takeoff power settings and the red crosshatched blocks for climb-power settings. The horizontal axis represents the airspeed in terms of Mach number and the vertical axis the altitude above mean sea level in feet. It is assumed that the aircraft will not exceed a Mach number of 0.35 below 2500 feet MSL. Between 2500 and 10,000 feet, the aircraft is limited to speeds below 0.46, which roughly corresponds to an airspeed of 250 knots (ATM speed limit below 10,000 feet MSL). As can be derived from the input blocks, airports until 6000 ft elevation are captured. In fact it is defined such that Denver International Airport, elevated at 5400 ft, can be used for fuel consumption modeling.

## 2.3 Generating TSFC/Thrust coefficients from data set

As has been explained in section 2.2, each calculated data point in PIANO contains thrust, fuel flow and TSFC values for both takeoff rating and climb rating. Each data set is filtered for both the takeoff and climb regimes. This filtering process is based on satisfying the conditions of each regime. These conditions are (see figure 2.2):

- For the takeoff regime: data points satisfying altitude  $\leq 8000$  ft and Mach  $< 0.4$
- For the climb regime: data points satisfying altitude  $\geq 1500$  ft and Mach  $> 0.2$

Based on this filtering, the thrust coefficients for both the climb and takeoff regime can be determined. When combining the filtered data sets, the full data set for departure operations is obtained where from the departure TSFC coefficients can be determined.

International Standard Atmosphere (ISA) equations, found in [2], are used to calculate the aircraft states (i.e. temperature, density and pressure) at each altitude point. The data extracting from the PIANO output files, the filtering of each data set, the processing of the data and the coefficient determinations are all performed using MATLAB [11].



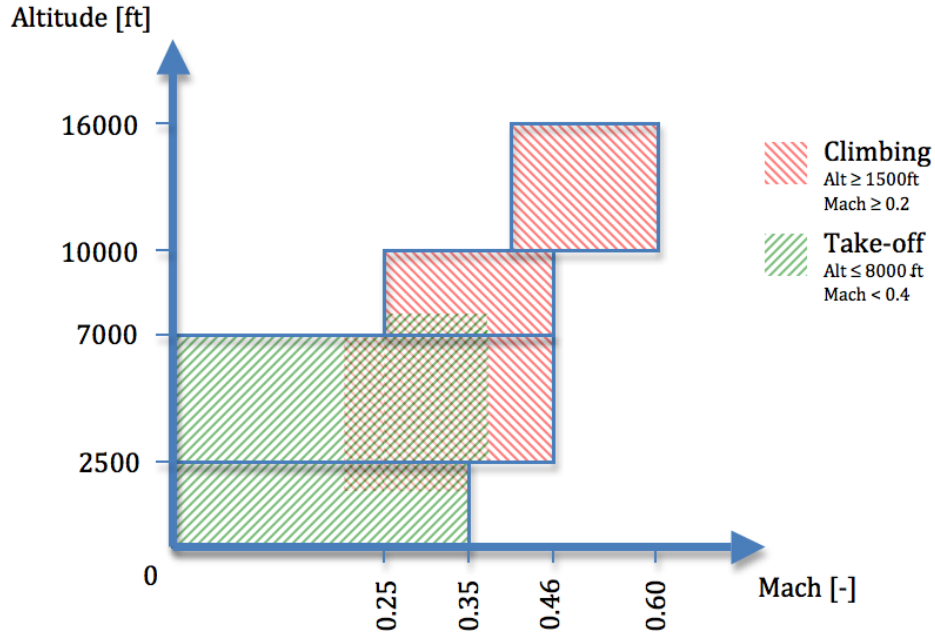


Figure 2.2: Departure data collection region

The unknown variables in equations 2.1 and 2.2 must be found in order derive their coefficients. First, the temperature and pressure ratio are calculated. The velocity is given as output in terms of the Mach number. Using a simple equation, the True Airspeed (TAS) can be derived from the Mach number. Since the velocity in equation 2.2 equals the Calibrated Airspeed, a conversion of TAS to CAS must be made. To establish this conversion, the density and pressure at aircraft altitude must be determined. These last two variables can be calculated using the temperature and pressure ratios. These derivations are performed step by step (step 1 through 5).

1. The temperature ratio can be calculated using

$$\theta = 1 + \frac{0.3048 \cdot \lambda \cdot h}{T_0} \quad (2.3)$$

where

- $\lambda$  the temperature lapse rate (-0.0065 Kelvin/m)
- 0.3048 conversion factor from feet to meter
- $h$  the aircraft altitude (ft) MSL
- $T_0$  the ISA temperature (288.15 Kelvin) at MSL

2. The pressure ratio is defined as the temperature ratio to the power 5.226, or

$$\delta = \theta^{5.226} = \left( 1 + \frac{0.3048 \cdot \lambda \cdot h}{T_0} \right)^{5.226} \quad (2.4)$$

3. From this the density and pressure at aircraft altitude can be determined using the following expressions

$$\rho = \rho_0 \cdot \left( 1 + \frac{0.3048 \cdot \lambda \cdot h}{T_0} \right)^{4.226} \quad (2.5)$$

$$P = P_0 \cdot \left( 1 + \frac{0.3048 \cdot \lambda \cdot h}{T_0} \right)^{5.226} \quad (2.6)$$

where

$P_0$  the pressure at sea level (101,325 N/m<sup>2</sup>)

$\rho_0$  the density at sea level (1.225 kg/m<sup>3</sup>)

4. The true airspeed depends on the Mach number and can be calculated as follows

$$V_{TAS} = M \cdot \sqrt{\gamma \cdot R \cdot T} \quad (2.7)$$

where

$\gamma$  the isentropic expansion coefficient for air = 1.4

$R$  the universal gas constant for air (287.05287 m<sup>2</sup>/K/s<sup>2</sup>)

$T$  the temperature (Kelvin) at aircraft altitude

5. Now, the velocity component in the thrust equation (see equation 2.2) is the calibrated airspeed  $V_{CAS}$ . The following expression can be used to convert the true airspeed to the calibrated airspeed

$$V_{CAS} = \left[ \frac{2 P_0}{\mu \rho_0} \left\{ \left( 1 + \frac{P}{P_0} \left[ \left( 1 + \frac{2 \rho}{\mu P} V_{CAS}^2 \right)^{\frac{1}{\mu}} - 1 \right] \right)^{\mu} - 1 \right\} \right]^{\frac{1}{2}} \quad (2.8)$$

where  $\mu = \frac{\gamma-1}{\gamma}$ .

### 2.3.1 Thrust coefficients determination

Once all the aircraft states from the thrust equation (equation 2.2) are determined, the thrust coefficients  $E$ ,  $F$ ,  $G_A$  and  $G_B$  for rated takeoff power and maximum climb power can be found using least squares method in MATLAB.

A list of the rated takeoff power and the maximum climb thrust coefficients for all the airplanes that were processed can be found in appendix A.

### 2.3.2 Departure TSFC coefficients determination

Combination of the filtered data sets of both the climb and takeoff regimes, gives the full departure operation data set. This full data set is required to determine the departure TSFC coefficients  $K_1$ ,  $K_2$ ,  $K_3$  and  $K_4$ . Also here, the least squares method in MATLAB can be applied to determine these coefficients.

The departure TSFC coefficients of all the processed aircraft are listed in appendix B.



## Chapter 3

# Departure Aerodynamic Coefficients

Before the AEDT software can determine the fuel consumption of an aircraft, three types of coefficients should be specified, i.e. TSFC, thrust and aerodynamic coefficients. For several aircraft, e.g. the Airbus A320 family, the aerodynamic coefficients as well as the thrust coefficients are already known and have been implemented in AEDT. This data originates from aircraft manufactures and provided for the FAA's legacy tools. Consequently for these aircraft PIANO is only used for the determination of the TSFC coefficients. For those aircraft without any data in the legacy tools, PIANO is used to generate thrust- and aerodynamic coefficients as well as the TSFC coefficients. The previous chapter discusses the generation of the TSFC and thrust (takeoff and maximum climb thrust) coefficients, since they are determined from the same PIANO data set. This chapter gives the determination of the aerodynamic coefficients. The departure aerodynamic equations are given in the first section. The next section explains the method to extract the required data from PIANO. Section 3.3 discusses the data processing steps.

### 3.1 Departure aerodynamic equations

There are three aerodynamic coefficients for departure: the initial-climb Calibrated Airspeed (CAS) coefficient  $C_f$ , the takeoff ground-roll coefficient  $B_f$  and the departure drag-over-lift coefficient  $R_f$ . They all depend on a particular flap setting. The departure aerodynamic equations are derived from the SAE-AIR-1845 document and they are defined by equations 3.1, 3.2 and 3.3, respectively [16]. Because of the flap setting dependence aerodynamic coefficients are often referred as flap coefficients. This term is not used in this report.

#### 3.1.1 Initial-climb calibrated airspeed coefficient $C_f$

During the initial climb it is assumed that the aircraft has an initial-climb airspeed which has a consistent relationship to fundamental aerodynamic lifting capability and hence to departure profile weight (release gross weight). This CAS is determined at takeoff screen height, which is 35 ft Above Ground Level (AGL). The initial-climb CAS coefficient  $C_f$  is calculated by equation 3.1.

$$C_f = \frac{v_i}{\sqrt{W}} \quad (3.1)$$

where

- $v_i$  CAS at initial climb (35 ft AGL), generally the aircraft speed  $v_2+15$  knots
- $W$  departure profile weight (lb), weight is assumed to remain constant during the entire takeoff

It is assumed that after liftoff the aircraft accelerates to an airspeed which is 15 knots higher than the aircraft safety speed  $v_2$ .

### 3.1.2 Takeoff ground-roll coefficient $B_f$

The takeoff ground-roll coefficient  $B_f$  is used to determine the ground roll distance  $S_g$  which is an approximation of the actual takeoff ground-roll. The coefficient is determined by the following equation.

$$B_f = \frac{S_g \cdot N \cdot \left(\frac{F_N}{\delta}\right)}{\theta \cdot \left(\frac{W}{\delta}\right)^2} \quad (3.2)$$

where

- $S_g$  ground-roll distance (ft), with zero degree runway slope
- $N$  number of engines supplying thrust
- $F_N/\delta$  corrected net thrust per engine (lbf) at takeoff screen height
- $\theta$  temperature ratio at takeoff screen height, MSL
- $W$  departure profile weight (lb)
- $\delta$  pressure ratio at takeoff screen height, MSL

The corrected net thrust is determined at the takeoff screen height, at this height it is assumed that the landing gear is retracted

### 3.1.3 Departure drag-over-lift coefficient $R_f$

The departure drag-over-lift coefficient  $R_f$  is used during climb segments, in which each segment is related to a particular flap setting. Additionally each climb segment is flown at a constant CAS (climbing from altitude  $h_1$  to  $h_2$ ).  $R_f$  is defined by equation 3.3.

$$R_f = \frac{N \cdot \left(\frac{F_N}{\delta}\right)_{avg}}{\left(\frac{W}{\delta_{avg}}\right)} - \frac{\sin \gamma}{K} \quad (3.3)$$

where

- $\left(\frac{F_N}{\delta}\right)_{avg}$  nominal value of the corrected net thrust per engine (lbf) of the related climb segment (mid-point value)
- $W$  aircraft gross weight (lb) at the start of the related climb segment
- $\delta_{avg}$  nominal value of the pressure ratio of the related climb segment (mid-point value)

|          |   |
|----------|---|
| $\gamma$ | average climb angle or flight path angle of the related climb segment                             |
| $K$      | speed-dependent constant $K = 1.01$ , when climb speed $\leq 200$ knots, and $K = 0.95$ otherwise |

As mentioned previously, aerodynamic coefficients depend on a particular flap setting. As a consequence, aircraft have an aerodynamic coefficient data set, i.e. each flap setting has a drag-over-lift ratio which is used for the related climb segment.

In order to calculate the aerodynamic coefficients for each individual aircraft, all the parameters which are situated at the righthand side of equations 3.1, 3.2 and 3.3 should be defined. The next section discusses the method to extract all the required parameters from PIANO.

### 3.2 Data generation using PIANO

In order to define all the required parameters, which are needed to calculate the aerodynamic coefficients, a flight maneuver is simulated in PIANO. PIANO can give data of the low speed drag polar at different flap settings. But this data is related to initial climb-out and to the safety speed, and so it is only valid for one flap setting (takeoff flap setting). Aerodynamic coefficients depend on among other thrust setting, aircraft weight and altitude. This data can only be extracted when a flight maneuver is simulated. An illustration of this function is given in figure 3.1.

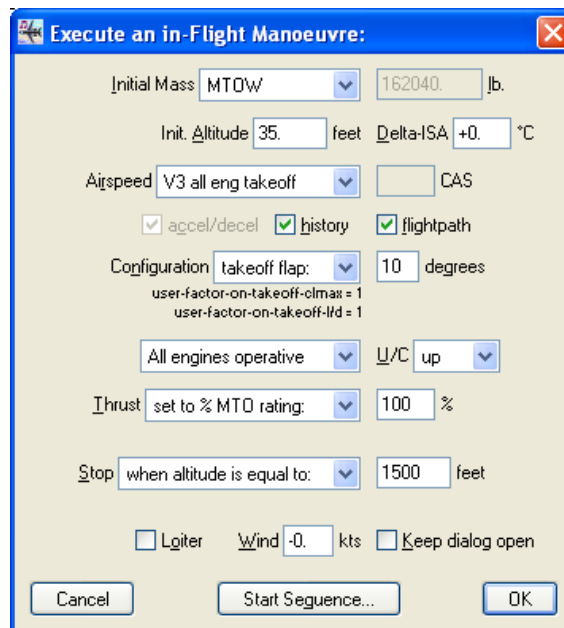


**Figure 3.1:** Example of the flight maneuver function in PIANO [8] showing the input entries

The flight maneuver function cannot be used directly because each aircraft has its own departure profile. Hence, this departure profile has to be defined first before any flight maneuver can be simulated in PIANO. It has to be noted that PIANO has a programmed standard departure, but this departure is insufficient since it assumes that each aircraft has only two departure flap settings (takeoff flap setting and zero flap setting). Consequently the standard

climb in PIANO is composed of two segments. First, the aircraft climbs to 1500 ft AGL using the takeoff configuration (constant CAS, takeoff flap setting and takeoff thrust). At 1500 ft flaps are retracted to zero degrees and the aircraft climbs further to 10,000 ft AGL using the maximum climb configuration (CAS set at 250 knots, zero flap setting and maximum climb thrust setting). However, most (jet) aircraft have multiple departure flap settings and so its departure is composed of multiple climb segments. As a result, a standard climb maneuver for each aircraft has to be defined first before the require date can be generated in PIANO. Unfortunately aircraft manufactures provide almost no information on how their aircraft are operated. As a consequence, the departure profiles which are defined in this report are developed by combining data of several sources like among others Flight Data Recorder (FDR) information, type certificate data sheets [13] (Federal Aviation Administration and Civil Aviation Authority) and Jane’s All the The World’s Aircraft [7]. The availability of FDR information from three Airbus aircraft, i.e. A330-200, A340-300 and A340-500, resulted in two different methods to define the departure profiles; FDR based departure and NOT-FDR based departures. Both departures are now explained.

### 3.2.1 FDR based departure profiles

The standard departure maneuver defined for the A330-200, A340-300 and A340-500 is based on its FDR data, since this data originates from actual flights. But it is also based on departure profiles from family aircraft, e.g. A330-300 and A330-200, which are already included in the current AEDT version. The reason why the standard departure maneuver is not only based on the FDR data is twofold. First, the FDR data for each aircraft consist of departures executed at one or two airports. The departure profile is aircraft and airport dependent. To derive a standard departure profile which is merely based on departures at one or two airports will likely result in a specified departure instead of a general departure. Secondly, this specification is resolved by having a study on standard departures of a family aircraft. The current AEDT version has standard departure profiles for the A330-300, A340-200 and A340-600. It is reasonable to assume that aircraft from the same family have similar departure profiles. Hence, standard departure profiles are derived based on departure profiles from family aircraft, combined with actual data (FDR). The departure templates of the A330-200, A340-300 and A340-500 are given in tables 3.1, 3.2 and 3.3, respectively.

**Table 3.1:** Departure template of the Airbus A330-200

|           | Flap angle [deg] | CAS [knots] | Final altitude [ft] | Thrust setting |
|-----------|------------------|-------------|---------------------|----------------|
| Segment 1 | 14               | $v_2 + 15$  | 2000                | Max takeoff    |
| Segment 2 | 8                | 195         | 3000                | Max climb      |
| Segment 3 | 0                | 250         | 10,000              | Max climb      |

**Table 3.2:** Departure template of the Airbus A340-300

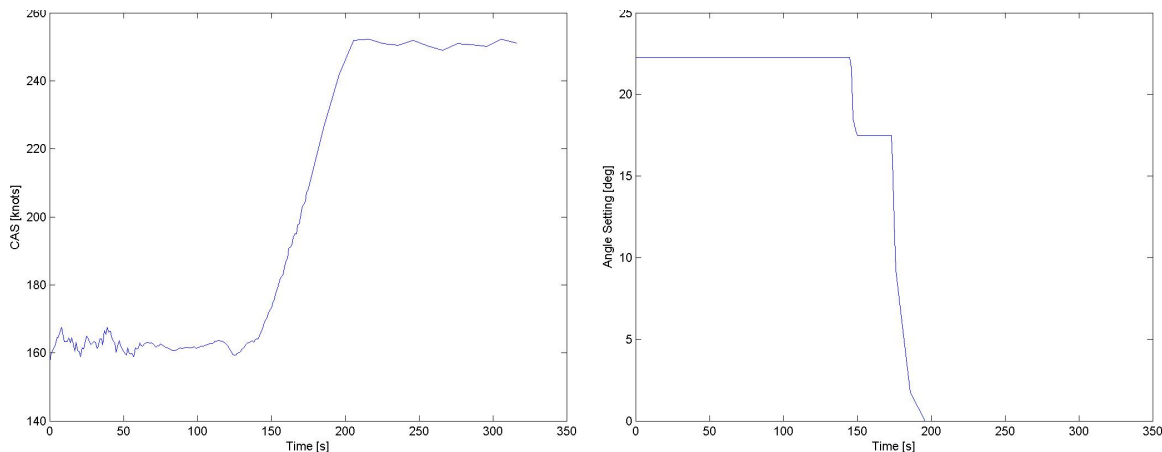
|           | Flap angle [deg] | CAS [knots] | Final altitude [ft] | Thrust setting |
|-----------|------------------|-------------|---------------------|----------------|
| Segment 1 | 22               | $v_2 + 15$  | 3000                | Max takeoff    |
| Segment 2 | 17               | 205         | 4000                | Max climb      |
| Segment 3 | 0                | 250         | 10,000              | Max climb      |

**Table 3.3:** Departure template of the Airbus A340-500

|           | Flap angle [deg] | CAS [knots] | Final altitude [ft] | Thrust setting |
|-----------|------------------|-------------|---------------------|----------------|
| Segment 1 | 22               | $v_2 + 15$  | 3500                | Max takeoff    |
| Segment 2 | 17               | 205         | 4500                | Max climb      |
| Segment 3 | 0                | 250         | 10,000              | Max climb      |

It has to be noted that the values and settings in tables 3.1, 3.2 and 3.3 are in fact not only based on FDR data and AEDT family aircraft but also on the input limitations of PIANO's flight maneuver function. PIANO can only execute a climb maneuver at constant CAS, in other words accelerations cannot be simulated. This has a specific effect on climb segment two.

Flaps are retracted on schedule when the aircraft accelerates gradually. This means that in reality the CAS during for instance climb segment two is not constant, as this can be derived from figure 3.2. The left graph of figure 3.2 gives the CAS while the right graph gives the flap position, both with respect to time, of an A340-500 departure (performed at Zurich Airport). When the two graphs are combined, it can be seen that the start and final CAS of the second flap position (17 degrees) are approximately 175 and 218 knots, respectively. This acceleration cannot be simulated in PIANO. Consequently, the CAS which is set as input in the flight maneuver function should be an averaged value. The liftoff speed of an aircraft which has a relative high TOW, will have in general higher airspeeds during the initial climb segments (the CAS of a jet aircraft during climb segment three will be 250 knots, since this is the ATM airspeed limit below 10,000 ft). Hence, jet aircraft which have a relative low or a relative high TOW will have averaged CAS of 195 or 205 knots during climb segment two, respectively. Which value is chosen should be carefully determined because it does not only effect the output values of PIANO. It also has an effect on the value of the speed-dependent constant  $K$ , see equation 3.3.

**Figure 3.2:** CAS (left) and flap angle (right) of FDR data from an A340-500 departure

### 3.2.2 NOT-FDR based departure profiles

The majority of aircraft that require the determination of aerodynamic coefficients have no FDR data available nor have family aircraft in the current AEDT version. Additionally, which



is already earlier quoted, aircraft manufactures give few information on how their aircraft are operated. As a result there is no actual source from which departure profiles can be derived. For those aircraft a general template is defined which can found in table 3.4.

**Table 3.4:** General departure template

|           | Flap angle [deg] | CAS [knots] | Final altitude [ft] | Thrust setting |
|-----------|------------------|-------------|---------------------|----------------|
| Segment 1 | F2               | $v_2 + 15$  | 1500                | Max takeoff    |
| Segment 2 | F1               | 195/205     | 3000                | Max climb      |
| Segment 3 | F0               | 250         | 10,000              | Max climb      |

Almost all aircraft, beside a few exceptions, are subjected to the template. The value for the CAS at segment two is determined by the TOW. More information on this CAS can be found in the previous subsection. At this moment there are three aircraft which have a deviation on the template, i.e. ATR 42-500, ATR 72-500 and Fokker F70. These aircraft have two departure flap settings, consequently the departure consists of two climb segments. Furthermore, the two ATR aircraft are both propeller driven and they cannot reach a CAS of 250 knots after flaps retraction. The standard CAS value of PIANO is used since no other source was found. The departure template of the ATR and of the Fokker aircraft can be found in tables 3.5 and 3.6, respectively.

**Table 3.5:** Departure template of the ATR 42-500 and ATR 72-500

|           | Flap angle [deg] | CAS [knots] | Final altitude [ft] | Thrust setting |
|-----------|------------------|-------------|---------------------|----------------|
| Segment 1 | 15               | $v_2 + 15$  | 1500                | Max takeoff    |
| Segment 2 | 0                | 146         | 10,000              | Max climb      |

**Table 3.6:** Departure template of the Fokker F70

|           | Flap angle [deg] | CAS [knots] | Final altitude [ft] | Thrust setting |
|-----------|------------------|-------------|---------------------|----------------|
| Segment 1 | 8                | $v_2 + 15$  | 1500                | Max takeoff    |
| Segment 2 | 0                | 246         | 10,000              | Max climb      |

The four variables of the departure templates i.e. flap angle, CAS, final altitude and thrust setting serve as input settings for the flight maneuver function of PIANO (figure 3.3). One climb maneuver is executed for each aircraft for which the start takeoff weight is set at MTOW, departure airport is elevated at 0 ft MSL and assuming that all engines operate at 100% thrust. The complete data output of an aircraft is composed of two or three successive climb maneuvers. Figure 3.3 gives the result of a PIANO output of one climb segment (each climb segment has the same format, only the values are different). The next section discusses the data output processing.

### 3.3 Data processing of PIANO output

The previous section gives a detailed explanation on the method to generate the required aerodynamic data. Except for the takeoff distance  $S_g$ , all variables of equations 3.1, 3.2 and 3.3 are determined from a climb maneuver output (figure 3.3). However, certain data requires processing before it can be substituted into the aerodynamic equations. This section explains the required processing as well as the determination of the takeoff distance.

```

Manoeuvre segment 1 starts at:
Initial Mass      507064.    lb. (CL 1.32 airbus)
Initial Altitude  35.      feet
Delta-ISA        +0.      degC
Airspeed (CAS)   170.     kts (v3)
Flaps            14      deg.
Undercarriage    up
All eng.operative
Thrust per engine 56216.    1bf. (100% MTO)

Climb/Descent rate 2415.    feet/min
Flightpath angle  8.0      deg. (grad.13.99%)
True airspeed     170.     kts

Fuel Flow rate    51024.    lb/hr
NOx emission rate 2635.5    lb/hr
HC emission rate  2.744     lb/hr
CO emission rate  18.6      lb/hr

L/D ratio         13.05
Total aircraft drag 38853.    1bf.

Segment 1 ends at total time = 0.8 mins, endmass = 506371.lb.

      Altitude   Time   Distance   Fuel Burn   NOx   HC   CO
      feet      sec   n.miles    lb.        lb.   lb.  lb.
Increm: +1965.  +49.9  +2.39     +692.2     +35.30 +0.038 +0.25
Final : 2000.  49.9   2.39      692.2     35.30  0.038  0.25
-----
History:  Alt   Time   Dist   Burnt   FN/eng   CAS   Mach   RoC
          35.   0.0   0.000   0.0     56216.  170.  0.258  2415.
          253.  5.4   0.258   76.9    55936.  170.  0.259  2404.
          472.  10.9  0.517   153.8   55656.  170.  0.260  2393.
          690.  16.4  0.779   230.7   55376.  170.  0.261  2381.
          908.  21.9  1.043   307.6   55097.  170.  0.262  2370.
          1127. 27.4  1.309   384.5   54818.  170.  0.263  2359.
          1345. 33.0  1.577   461.4   54539.  170.  0.264  2347.
          1563. 38.6  1.847   538.3   54261.  170.  0.265  2336.
          1782. 44.2  2.120   615.2   53983.  170.  0.266  2324.
          2000. 49.9  2.394   692.2   53705.  170.  0.267  2312.
-----

```

Figure 3.3: Output example of flight maneuver in PIANO

The initial-climb speed coefficient  $C_f$  (equation 3.1) is determined from the first climb segment (takeoff flap setting). The weight  $W$  is defined as the MTOW (in figure 3.3 it is given as the initial mass) and the CAS at 35 ft AGL, i.e.  $v_i$ , is found in the *History* part of the data output. Within the first climb segment it does not matter from which altitude  $v_i$  is determined, since the climb is performed at constant CAS. If the data output is figure 3.3 thoroughly studied, it can be seen that within PIANO  $v_i$  is defined as  $v_3$ .

The takeoff ground-roll coefficient  $B_f$  (equation 3.2) is also determined from the first climb segment. The temperature and pressure ratio, equations 2.3 and 2.4 respectively, are calculated at 35 ft MSL. The values are almost equal to one. In the same way as it was defined for the initial-speed coefficient, the weight  $W$  in equation 3.2 is defined as the MTOW. The takeoff distance is the last variable which has to be defined (the number of engines  $N$  can be considered as a known constant). This variable can be determined from the takeoff field function (TOFL) in PIANO. It gives the TOFL for different TOW at a particular flap setting (takeoff flap setting). Logically the TOFL from MTOW is taken since the aerodynamic coefficients are determined with respect to this weight. PIANO defines TOFL as the distance from the start of the takeoff roll until 35 ft above the runway. The takeoff distance is calculated from the TOFL by using the following equation 3.4.

$$S_g = \text{TOFL} - \frac{35}{\tan \gamma} \tag{3.4}$$

where

- $\gamma$  flight path angle during climb segment one
- TOFL takeoff field length (ft)

The drag-over-lift coefficient, equation 3.3, is determined for each departure flap settings (all climb segments). Whereas the initial-climb speed coefficient and takeoff ground-roll coeffi-

cient are only determined for the highest departure flap setting (first climb segment, takeoff flap setting); since it is reasonable to assume that aircraft always use this setting for takeoff. Hence the second and third climb segments are only used to determine the drag-over-lift coefficients for the particular flap setting. Both procedures are the same as for the first climb segment, which is explained below. The value of the weight  $W$  is directly given as the initial weight in PIANO's output. Note that this value is lower for segment two and three since at this point, a certain amount of fuel has been consumed. The flight path angle is also directly extracted from the output file.

In order to calculate the nominal corrected net thrust and the nominal pressure ratio, see equation 3.3, the pressure ratio is first determined at the start and final altitude (35 ft and 1500 ft in figure 3.3). The nominal pressure can then be determined directly by taking the average of both values. To calculate the nominal corrected net thrust, first the corrected net thrust at the start and final altitudes are determined. Then the average of both values is taken.

All process steps are defined, and the coefficients are determined using MATLAB. The results, i.e. the aerodynamic coefficients, can be found in appendix C.

## Chapter 4

# Arrival TSFC Coefficients

Chapter 2 explains the determination of the departure TSFC coefficients. The equation which is used to determine these coefficients can not be used for arrival operations. At low thrust values, TSFC has an exponential relationship with corrected net thrust. The equation that is used to derive the arrival TSFC coefficients is introduced in section 4.1. In section 4.2, it is explained how the data (required to determine the arrival TSFC coefficients) is generated using the software tool PIANO. Finally, the data processing procedure and the method to find these coefficients are discussed in section 4.3.

### 4.1 Arrival TSFC equation

The following TSFC equation for arrival operations in the terminal area is based on the work by Hill [5] and modifications by Yoder [19],

$$\frac{\text{TSFC}}{\sqrt{\theta}} = \alpha + \beta_1 \cdot M + \beta_2 \cdot e^{-\beta_3 \cdot \left(\frac{F_N}{\delta \cdot F_0}\right)} \quad (4.1)$$

where

|                                     |  |
|-------------------------------------|--|
| $M$                                 | aircraft Mach number   |
| $\frac{F_N}{\delta}$                | corrected net thrust per engine (lbf)                                  |
| $F_0$                               | the maximum thrust at sea level static condition (lbf)                 |
| $\theta$                            | temperature ratio (altitude dependent)                                 |
| $\alpha, \beta_1, \beta_2, \beta_3$ | regression coefficients to be determined for individual airplane types |

The regression coefficients for each airplane/engine combination are found by generating data for a wide range of operational conditions, collecting this data into an organized structure and then statistically analyzing it. The data generation is discussed in section 4.2.

### 4.2 Data generation using PIANO

The data generation for the arrival TSFC coefficients is similar to the procedure for the departure operations data generation. The only difference here lies in the inputs for the *point performance function* in PIANO. Next to the aircraft altitude and Mach number inputs, thrust is given as a third input. The input combinations for ranging Mach number, aircraft

operating altitudes and ranging thrust values are shown in table 4.1. The same inputs are used for propelled airplanes. The Mach number and altitude ranges are also graphically represented by figure 4.1.

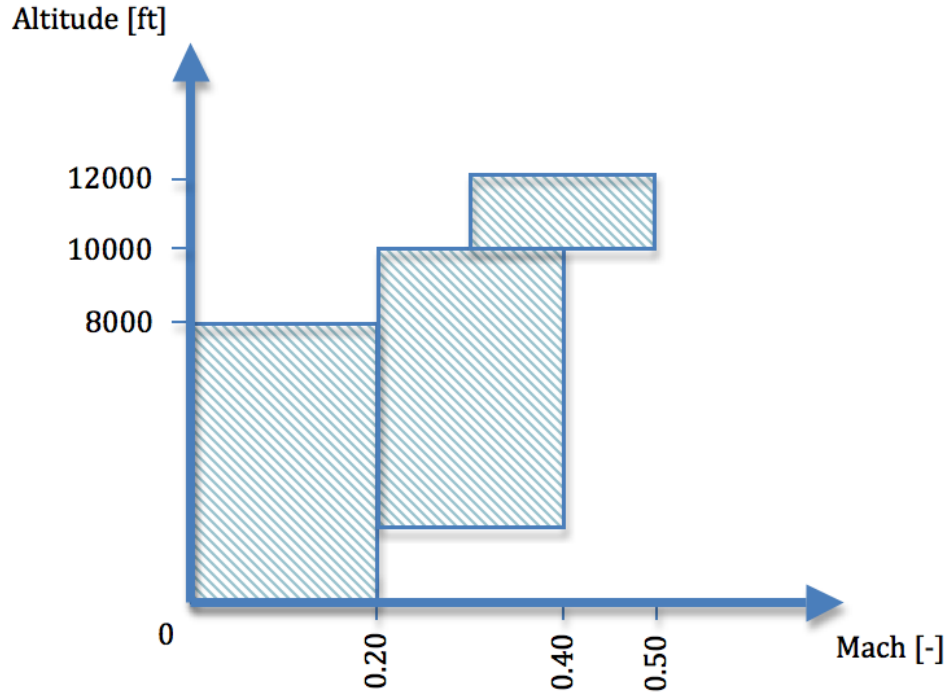


Figure 4.1: Arrival data collection region

Table 4.1: Point performance function (Piano) inputs for arrival operations

|         | Mach number [-]           | Altitude [ft]                   | Thrust [lbf]               |
|---------|---------------------------|---------------------------------|----------------------------|
| Block 1 | 0 – 0.2 (steps of 0.1)    | 0 – 8000 (steps of 2000)        | 500 – $F_0$ (steps of 250) |
| Block 2 | 0.2 – 0.4 (steps of 0.05) | 2000 – 10,000 (steps of 2000)   | 500 – $F_0$ (steps of 250) |
| Block 3 | 0.3 – 0.5 (steps of 0.1)  | 10,000 – 12,000 (steps of 2000) | 500 – $F_0$ (steps of 250) |

The thrust input ranges from 500 lbf to the maximum thrust at sea level condition of an airplane. Not all these data points will be used since a filtering on the data set will be applied (see next section). The data generation using the point performance function in PIANO, is automated using WINBATCH [18].

### 4.3 Generating arrival TSFC coefficients from data set

The generated data is first collected into a organized structure using MATLAB. Then, a selection is made on the data points that satisfy following conditions:

- $TSFC < TSFC_{lim} = 1.1$  – higher TSFC values are left out to avoid an upward shift of the TSFC curves in figure 4.2 which may cause problems in the determination of the arrival coefficients

- $0 < \frac{F_N}{\delta \cdot F_0} < 0.6$  – this condition is deduced from figure 4.2 where the curves ranging from 0 to 0.6 on the horizontal axis represent arrivals, whereas larger values represent departures (see departure TSFC equation where the coefficients are linearly dependent on the aircraft states)

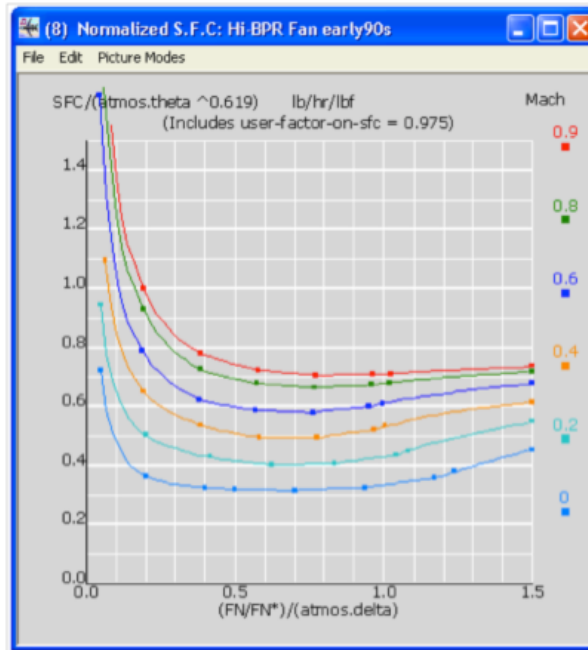


**Figure 4.2:** TSFC loops (Engine characteristics, PIANO [8])

Once the data is filtered (satisfying conditions), the data can be processed. The temperature ratio  $\theta$  and pressure ratio  $\delta$  for each data point are calculated using equations 2.3 and 2.4. Next, the arrival TSFC coefficients are determined using a multiple non-linear regression function from the statistical software analysis tool STATISTICA [17]. The calculated coefficients can be found in appendix C.



## Chapter 5

# Arrival Aerodynamic Coefficients

AEDT uses several aircraft specific aerodynamic coefficients in its simulations, as this is explained in chapter 3. AEDT uses three aerodynamic coefficients for departures, while for arrival simulations it only uses two:  $R_f$  and  $D_f$ , both dependent on flap and landing gear settings. The  $R_f$  coefficient is a value for the drag-over-lift ratio, the  $D_f$  coefficient is used to calculate the landing speed. In this chapter, the methods used to determine these coefficients from extracted PIANO data will be explained. The departure aerodynamic equations are given in the first section. The data generation and processing is explained in section 5.2.

### 5.1 Arrival aerodynamic equations

In this section the equations for both aerodynamic coefficients, derived from the SAE-AIR-1845 document [16], are introduced and their parameters are explained.

#### 5.1.1 Arrival drag over lift coefficient $R_f$

As stated before, AEDT uses values for  $R_f$  and  $D_f$  in its simulations. In particular,  $R_f$  is used to calculate the thrust needed, assuming a known value for descend angle  $\gamma$ . For a descend segment the following equation is used to calculate  $R_f$ :

$$R_f = \left( \frac{F_N}{\delta} \right)_2 \cdot \left( \frac{\delta_2}{W} \right) \cdot N + \frac{\sin \gamma}{1.03} \quad (5.1)$$

where

- $\left( \frac{F_N}{\delta} \right)_2$  corrected net thrust per engine at the end of the arrival segment (lbf)
- $W$  profile weight (lbs)
- $\delta_2$  pressure ratio at the altitude of the end of the arrival segment
- $\gamma$  average descend angle (degrees, positive value)
- $N$  number of engines supplying thrust

The pressure ratios cancel each other out and equation 5.1 is simplified to:

$$R_f = \left( \frac{F_N}{W} \right)_2 \cdot N + \frac{\sin \gamma}{1.03} \quad (5.2)$$



### 5.1.2 Landing speed coefficient

$D_f$  is a coefficient used by AEDT to calculate the landing speed. For a landing segment in AEDT the following equation is used:

$$D_f = \frac{V_1}{\sqrt{W}} \quad (5.3)$$

where

$V_1$  calibrated airspeed (knots) just before landing

## 5.2 Data generation using PIANO and data processing

PIANO is used to extract all variables on the righthand side of both equations. The *final approach* function under the *flight* tab in PIANO allows the user to input different weights, different flap and landing gear settings. Figure 5.1 below shows the *final approach* window, which in fact is similar to the *flight maneuver* function used to determine the departure aerodynamic coefficients (figure 3.1), only now more specified for arrival operations.

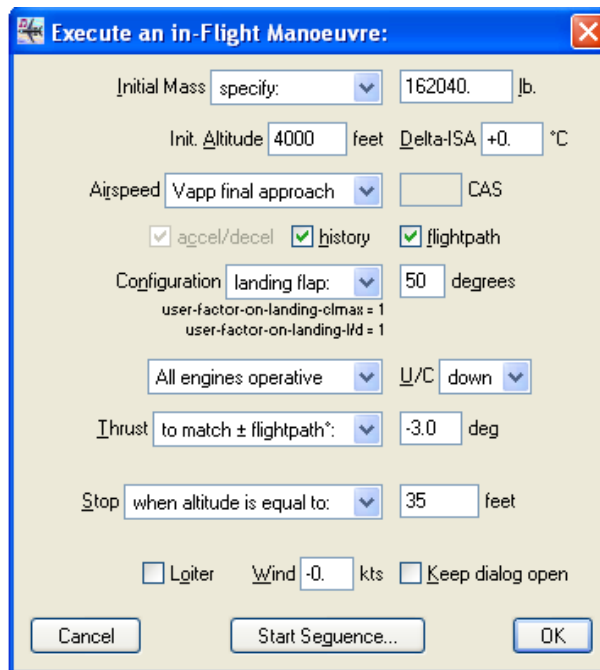


Figure 5.1: The Final Approach maneuver function in PIANO [8]

From type certification data sheets [13], FDR data and other sources common flap deflection angles are defined, and categorized under the following Flap ID labels: FULL\_D, 3\_D, 2\_D, 2\_U and ZERO. Each of these labels represents a certain flap deflection/landing gear setting combination. Using these flap deflections and landing gear settings, together with the normal landing weight (NLW) and assuming a glide slope of 3 degrees, the arrival simulation in PIANO is executed. The output of PIANO then gives the required thrust for those settings, as well as the CAS and other variables in equations 5.2 and 5.3.

As an example, different flap/landing gear combinations with their yielded variables and calculated coefficients for the A318-100 are shown in table 5.1 below:

**Table 5.1:** Example of calculated coefficients for flap/landing gear combinations of the A318-100

| Flap ID | Gear | Flap defl. [deg] | CAS [kts] | $W$ [lb] | $F_N$ [lbf] | $D_f$     | $R_f$     |
|---------|------|------------------|-----------|----------|-------------|-----------|-----------|
| FULL_D  | Down | 40               | 122       | 114,432  | 5757        | 0.3606501 | 0.1514303 |
| 3_D     | Down | 20               | 133       | 114,432  | 3003        | 0.3931678 | 0.1032969 |
| 2_D     | Down | 15               | 137       | 114,432  | 2324        | -         | 0.0914296 |
| 2_U     | Up   | 15               | 137       | 114,432  | 1555        | -         | 0.0779893 |
| ZERO    | Up   | 0                | 151       | 114,432  | 1275        | -         | 0.0561670 |

Note that the column containing the flap deflection angles serves as an input for the PIANO ‘Final Approach’ function, but that the values vary for different types of aircraft since they all fly using different flap angles.

The  $D_f$  and  $R_f$  coefficients are calculated as described in equations 5.2 and 5.3. The  $D_f$  coefficient is only calculated for the labels FULL\_D, and 3\_D, since the aircraft always lands using one of those settings.

Also, the  $R_f$  coefficient for the ZERO setting is calculated using a glide slope of 2 degrees, since PIANO is unable to perform the simulation using a glide slope of 3 degrees.

This process is carried out for all required aircraft. The calculated coefficients can be found in appendix C.



## **Part II**

# **Validation of PIANO Data with FDR Information**



## Chapter 6

# Departure Operations

This chapter validates the departure coefficients which are determined in Part I. It is an essential part in the development of the AEDT since it concerns two aspects. First, the validation gives understanding on the reliability of PIANO (third-party aircraft performance tool) in the terminal area. Second, the determined coefficients and the related extraction method in PIANO has to be validated. It is possible that inferior results are imputed to errors in the extraction method. This is especially related to the developed standard climb maneuver templates which are defined in chapter 3.

Flight Data Recorder (FDR) information – available for a number of Airbus aircraft – were used to validate the usage of PIANO for developing the TSFC, thrust and aerodynamic coefficients. Validation is conducted by comparing in-service fuel consumption data to the predicted fuel consumption (AEDT). FDR data was available to validate the departure model for the A319-100, A320-200, A321-200, A330-200, A340-300 and A340-500. The first three aircraft require validation of TSFC coefficients only while the last three aircraft require validation of TSFC, thrust and aerodynamic coefficients. As a result the validation is divided into two parts. In the first section the validation is given for aircraft with manufacturer provided aerodynamic coefficients. The second section validates aircraft with PIANO generated aerodynamic coefficients. A summary of the results and conclusions are found in the final section.

### 6.1 Validation of aircraft with manufacturer provided aerodynamic coefficients

The aircraft state parameter inputs for the TSFC equation, equation 2.1, are found in the FDR data. In other words, for each point in time, the values for  $M$ ,  $h$  and  $F_N$ , could come from the FDR. The temperature and pressure ratio are determined from altitude  $h$ , as a result the fuel flow  $\dot{m}_f$  can be determined by using equation 6.1.

$$\dot{m}_f = \text{TSFC} \cdot F_N \quad (6.1)$$

The FDR also reports the actual fuel flow of the airplane, allowing a direct comparison between the modeled and actual fuel flows. However, the thrust of an aircraft is not directly measured; the thrust is derived from other parameters (e.g. engine rotation speed, Mach

number, altitude, etc). The way the thrust is calculated in the FDR is unknown; comparisons with Boeing's BCOP model showed the FDR thrust is not accurate and reliable enough to perform a sound validation [15].

Therefore, to validate the generated TSFC coefficients, another method was used. The AEDT software was used to simulate different departure procedures, generating the required values for  $M$ ,  $h$  and  $F_N$ . Instead of comparing the fuel flow at a certain point in time for a particular flight, the total amount of fuel consumed was calculated for different departure procedures until 10,000 ft AGL. Each departure uses a different TOW (standard TOW in AEDT software), so that a relationship could be developed showing the amount of fuel consumed versus the TOW for both the FDR data and the AEDT-modeled departures. This has the advantage of showing the nominal as-modeled fuel consumption for a standard AEDT operation compared to actual fuel consumption for that modeled aircraft. The validation results for each aircraft, i.e. A319-100, A320-200, A321-200, are now given.

### 6.1.1 Validation of A319-100

The TSFC coefficients of the A319-100 are validated with FDR data originating from Swiss A319-112 aircraft. They all departed at Zurich Airport (LSZH) which is elevated at 1416 ft. The AEDT software is used to simulate departure procedures for five different takeoff weights (125,000 lb, 131,000 lb, 136,500 lb, 146,100 lb and 166,400 lb). The simulations are performed for an initial climb to 10,000 ft AGL and the output of an AEDT simulation contains, among others, true airspeed, corrected net thrust, altitude and time step duration (an example output can be found in Appendix D).

At each time step the Mach number is first calculated by using equation 2.7. The fuel flow at each time step is then determined by using equations 2.1 and 6.1. Finally, the total fuel consumption is calculated by taking the sum the fuel consumption at each time step which is determined by multiplying a time duration with its related fuel flow. Figure 6.1 shows the fuel consumption of an initial climb up to 10,000 feet as a function of takeoff weight.

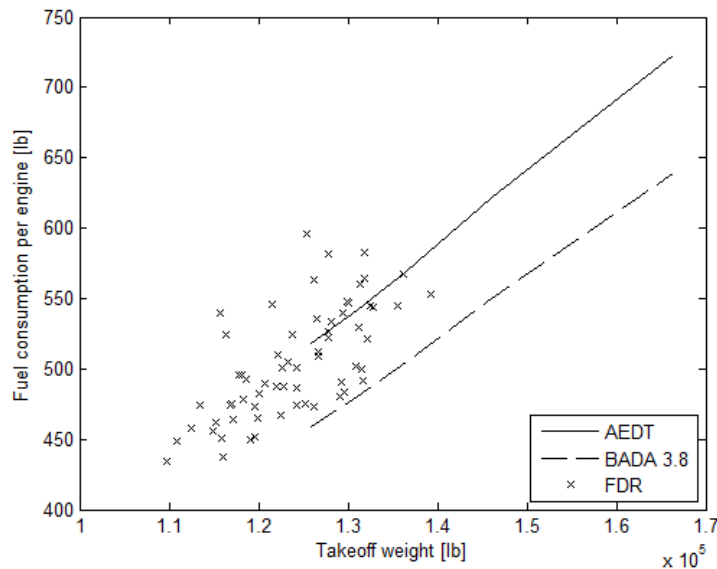


**Figure 6.1:** A319-100 validation for initial climb to 10,000 ft AGL, no extra TOW

Two curves are found in figure 6.1. The continuous line represents AEDT, the line is created

by connecting the fuel consumptions from each TOW. The dashed line represents BADA 3.8 (old method). Both lines are created from the same AEDT departure simulation. The fuel consumption for BADA 3.8 does not use equation 2.1 for the determination of TSFC, instead it uses the following equation [2].

$$TSFC = C_{f_1} \cdot \left(1 + \frac{V_{TAS}}{C_{f_2}}\right) \quad (6.2)$$

$C_{f_1}$  and  $C_{f_2}$  are TSFC coefficients (like the  $K$  coefficients from the AEDT algorithm), values for each aircraft are found in [1].  $V_{TAS}$  is the true airspeed which is extracted from the AEDT simulation output. Again referring to the two curves in figure 6.1, the difference is only created by a different TSFC equation. Without any error calculation it can already be stated that, by looking at the figure, the AEDT method (new method) shows, with respect to the BADA method (old method), an improvement in modeling the fuel consumption. However an exact error determination is still essential.

Curve fitting is needed to determine the error of both models. But due to fact that both models do not cover the complete FDR data set (lowest TOW of the model is 125,000 lb while the lowest TOW of FDR is approximately 110,000 lb). It is chosen to first make an additional departure in AEDT and then do the curve fitting, instead of doing the curve fitting directly. An additional departure is made for a TOW of 110,000 lb. Linear extrapolation from the previous two TOW, e.g. 125,000 lb and 131,000 lb, is used to determine the climb rates and CAS of the new TOW. The result of this extrapolation can be seen in figure 6.2.

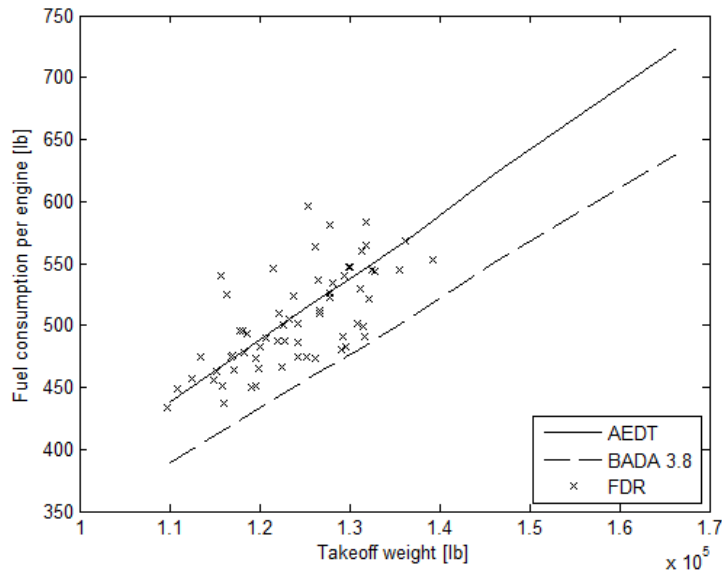


**Figure 6.2:** A319-100 validation for initial climb to 10,000 ft AGL, with extra TOW at 110,000 lb

After the linear extrapolation, the curve is fitted in MATLAB by using the second degree polynomial fit function. No linear fit is used, because this is not possible in theory. Logically a heavier aircraft requires more fuel than a lighter aircraft to travel the same range. Relatively, the heavier aircraft requires an additional amount of fuel because fuel is burned to transport fuel. This is simulated by the AEDT software by a (small) increase in gradient after 140,000 lb. A second degree polynomial fit can incorporate the change in gradient. Figure 6.3 shows the curve fit result of the A319-100.



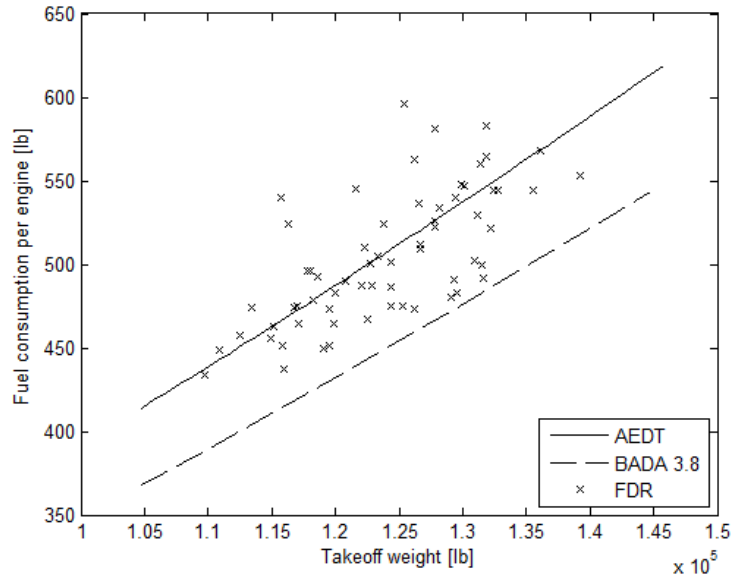


**Figure 6.3:** Curve fit result for the A319-100, initial climb to 10,000ft AGL, extra TOW at 110,000 lb

After the second degree polynomial fit it is possible to determine the error of both models with respect to the FDR. The takeoff weights of the FDR are all substituted into the polynomial fit equation. This gives the value of the modeled fuel consumption. The error of one takeoff weight is determined by equation 6.3.

$$\text{Error} = \frac{\text{FDR Fuel Consumption} - \text{Modeled Fuel Consumption}}{\text{FDR Fuel Consumption}} \quad (6.3)$$

An error is determined for each FDR data point. The average error for the A319-100 can be found in table 6.1.

**Table 6.1:** Average error of A319-100 validation

|                    | AEDT  | BADA 3.8 |
|--------------------|-------|----------|
| Average error in % | 0.853 | -10.572  |

From table 6.1 it can be seen that, as it was clearly noticeable in the figures, the AEDT method shows an improvement in fuel consumption modeling. The new method has a relative small overestimation, i.e. 0.85%, while the old method has a relative high underestimation, i.e. -10.57%.

### 6.1.2 A320-200 validation

The TSFC coefficients of the A320-200 are validated with FDR data from Swiss A320-214 aircraft which also departed from LSZH. The AEDT software is used to simulate five different departures. Departures are simulated until 10,000 ft AGL. As with the A319-100, the FDR data of the A320-200 is not completely covered by the takeoff weights given in AEDT. Hence an additional departure is simulated for a TOW of 125,000 lb. The result of the second order polynomial fit can be found in figure 6.4. The average error can be found in table 6.2. Please note that the validation procedure of the A320-200 is completely the same as the

one of the A319-100. More information on AEDT output, extra TOW, linear extrapolation, second order polynomial fit and error determination can therefore be found in the section of the A319-100 validation.

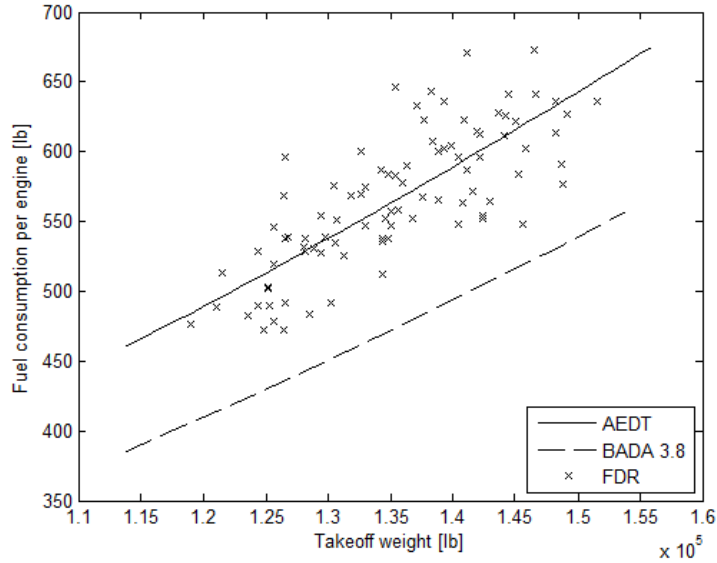


**Figure 6.4:** Curve fit result for the A320-200, initial climb to 10,000 ft AGL, extra TOW at 125,000 lb

**Table 6.2:** Average error of A320-200 validation

|                    | AEDT  | BADA 3.8 |
|--------------------|-------|----------|
| Average error in % | 0.207 | -16.013  |

The validation results of the A320-200 are in the same trend as of the A319-100. The AEDT method results in a relative small overestimation while the BADA method has a relative high underestimation.

### 6.1.3 A321-200 validation

The TSFC coefficients of the A321-200 are validated with FDR data originating from Swiss A321-111 aircraft which also departed from LSZH. The AEDT software is used to simulate five different departures. Departures are simulated until 10,000 ft AGL. As with the A319-100, the FDR data of the A321-200 is not completely covered by the takeoff weights given in AEDT. Hence an additional departure is simulated for a TOW of 130,000 lb. The result of the second order polynomial fit can be found in figure 6.5. The average error can be found in table 6.3. Please note that the validation procedure of the A321-200 is completely the same as the one of the A319-100. More information on AEDT output, extra TOW, linear extrapolation, second order polynomial fit and error determination can therefore be found in the section of the A319-100 validation.

**Table 6.3:** Average error of A321-200 validation

|                    | AEDT   | BADA 3.8 |
|--------------------|--------|----------|
| Average error in % | -5.203 | -14.093  |

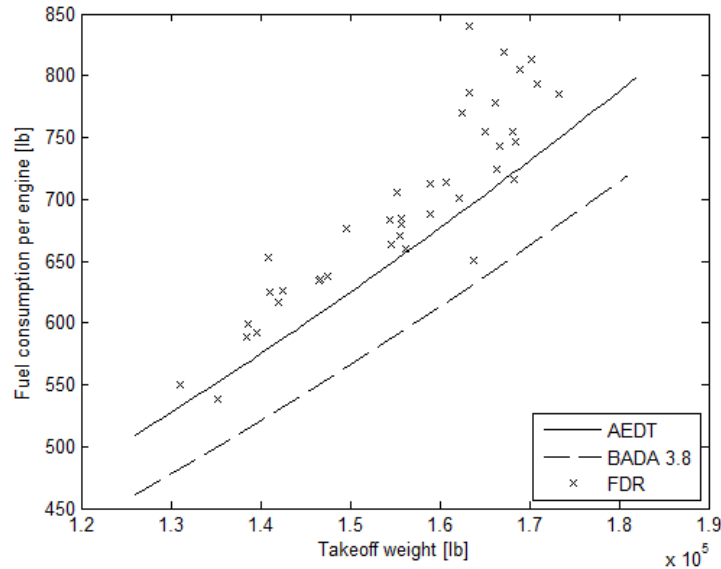


**Figure 6.5:** Curve fit result for the A321-200, initial climb to 10,000 ft AGL, extra TOW at 130,000 lb

From table 6.3 it can be seen that both models underestimate the fuel consumption of the A321-200. The error of the AEDT method is once again smaller than the one of the BADA 3.8 method.

## 6.2 Validation of airplanes with PIANO generated aerodynamic coefficients

The Airbus A330-200, A340-300 and A340-500 airplanes are, as mentioned previously, not implemented in the current AEDT version. As a consequence, aerodynamic and thrust coefficients are determined from data which is extracted from PIANO. More information on the extraction can be found in chapters 2 and 3. Both coefficients are required to simulate a departure with AEDT software. The problem is that there are no standard departures in the current AEDT software since these aircraft are not implemented. However, simulated departures are necessary to define  $M$ ,  $h$  and  $F_N$  which are required to determine the TSFC of an aircraft. It is reasonable to assume that aircraft from the same family have corresponding departure profiles. Therefore it is chosen to use standard departures of a family aircraft; e.g. standard departures of the A330-300 (implemented aircraft in AEDT) are used for the A330-200.

The thrust and aerodynamic coefficients are changed to the values of the A330-200. The previous section validates aircraft for which only TSFC coefficients are determined. Excellent results are obtained. Hence it is possible to state that TSFC coefficients have sufficient fidelity. The aircraft in this section require validation of three types of coefficients. However the same method of validation is applied, which is in fact a validation of the complete model (TSFC, thrust and aerodynamic coefficient). Hence, the validation in this section gives more understanding on the fidelity of the thrust and aerodynamic coefficients since it is already known that the TSFC coefficients have sufficient fidelity. The validation of the A330-200, A340-300 and A340-500 aircraft is now given.

### 6.2.1 A330-200 validation

The TSFC, thrust and aerodynamic coefficients of the A330-200 are validated with FDR data originating from Etihad A330-202 aircraft and Etihad A330-243 aircraft. The majority of these flights departed at Abu Dhabi International Airport (OMAA) which is elevated at 88 ft. The other airports are elevated at approximately 100 ft.

The AEDT software is used to simulate seven different departure. Departures are simulated until 10000 ft AGL. As with the A319-100, the FDR data of the A330-200 is not completely covered by the takeoff weights given in AEDT. Hence an additional departure is simulated for a TOW of 310,000 lb. The result of the second order polynomial fit can be found in figure 6.6. The average error can be found in table 6.4. Please note that the validation procedure of the A330-200 is completely the same as the one of the A319-100. More information on AEDT output, extra TOW, linear extrapolation, second order polynomial fit and error determination can therefore be found in the subsection of the A319-100 validation.

The AEDT method gives the best modeled fuel consumption for terminal area operations of the A330-200. This method has an underestimation of -3.88%, while the BADA 3.8 method has an underestimation of -9.82%.

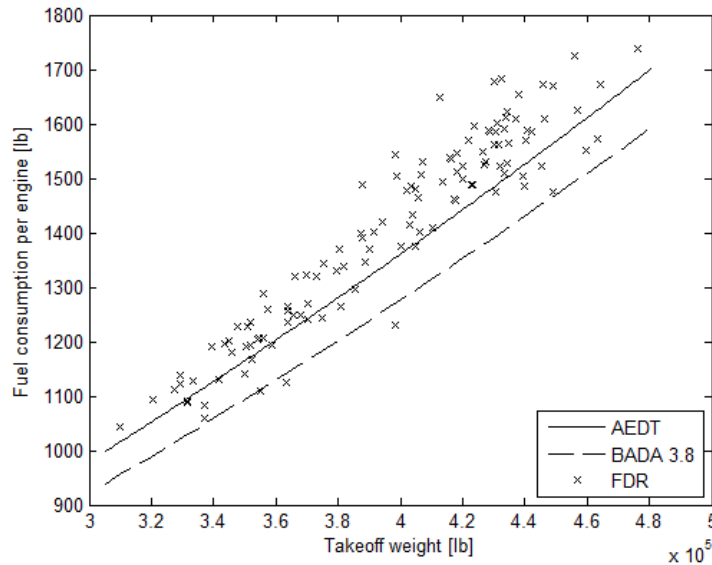


Figure 6.6: Curve fit result for the A330-200, initial climb to 10,000 f t AGL, extra TOW 310,000 lb

Table 6.4: Average error of A330-200 validation

|                    | AEDT   | BADA 3.8 |
|--------------------|--------|----------|
| Average error in % | -3.883 | -9.817   |

### 6.2.2 A340-300 validation

The TSFC, thrust and aerodynamic coefficients of the A340-300 are validated with FDR data from Swiss A340-313 aircraft which all departed from Zurich Airport. The departure profiles of the Swiss aircraft deviated from a more or less standard departure. Above 6000 ft AGL, the aircraft accelerated above the ATM speed limit (250 knots) and certain number of

aircraft performed a 360° turn. As a consequence the actual fuel consumption was higher than the one modeled in AEDT or BADA 3.8, since the AEDT software only simulates standard (ideal) departures. A conclusive validation is performed by simulating departures until 3000 ft AGL. Subsequently, no additional departure had to be made in AEDT since FDR data was completely covered by the takeoff weight in AEDT.

The result of the second order polynomial fit can be found in figure 6.7. The average error can be found in table 6.5. Please note that the validation procedure of the A330-200 is completely the same as the one of the A319-100. More information on AEDT output, extra TOW, linear extrapolation, second order polynomial fit and error determination can therefore be found in the section of the A319-100 validation.

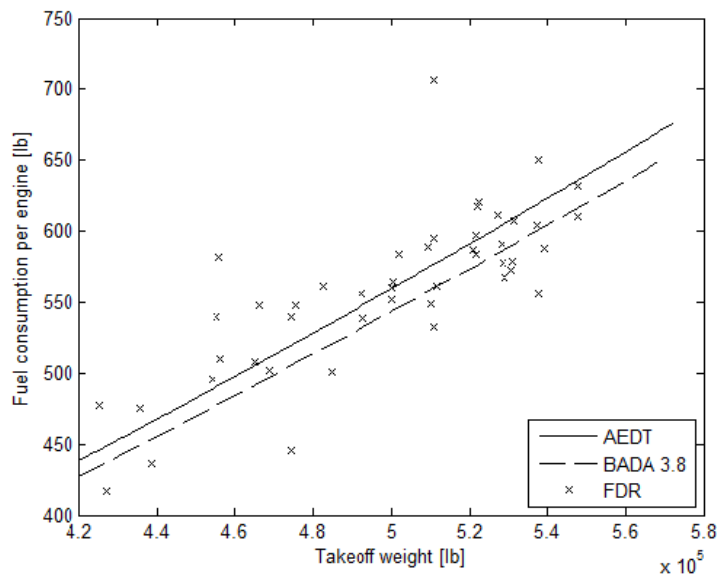


**Figure 6.7:** Curve fit result for the A340-300, initial climb to 3000 ft AGL, without extra TOW

**Table 6.5:** Average error of A340-300 validation

|                    | AEDT  | BADA 3.8 |
|--------------------|-------|----------|
| Average error in % | 0.163 | -2.739   |

From table 6.5, it can be seen that both methods, i.e. AEDT and BADA 3.8, perform very well. AEDT has an overestimation of 0.16%, BADA 3.8 has an underestimation of -2.74%. Both errors are relatively small. When previous errors of BADA 3.8 are compared with the error in table 6.5, it is remarkably that this error is relatively low. This gives the impression that the BADA 3.8 method is accurate within the control zone of the airport (CTR), but its accuracy decreases gradually when the aircraft continues its climb in the terminal area. However, this statement is only based on one fuel consumption modulation until 3000 ft. More examples are required to make it a solid statement.

### 6.2.3 A340-500 validation

The TSFC, thrust and aerodynamic coefficients of the A340-500 are validated with FDR data originating from Etihad A340-541 aircraft. The majority of these flights departed from

OMAA which is elevated at 88 ft. The other airports are elevated at approximately 100 ft.

The AEDT software is used to simulate seven different departures. Departures are simulated until 10,000 ft AGL. As with the A319-100, the FDR data of the A340-500 is not completely covered by the takeoff weights given in AEDT. Hence an additional departure is simulated for a TOW of 450,000 lb. The result of the second order polynomial fit can be found in figure 6.8. The average error can be found in table 6.6. The validation results of the A340-500 are in the same trend as for the previous aircraft.

Please note that the validation procedure of the A340-500 is completely the same as the one of the A319-100. More information on AEDT output, extra TOW, linear extrapolation, second order polynomial fit and error determination can therefore be found in the section of the A319-100 validation.

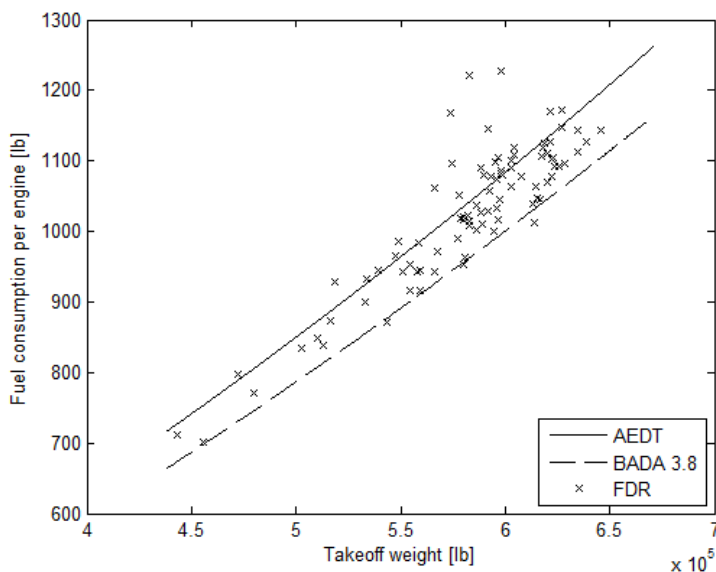


Figure 6.8: Curve fit result for the A340-500, initial climb to 10,000 ft AGL, extra TOW at 450,000 lb

Table 6.6: Average error of A340-500 validation

|                    | AEDT  | BADA 3.8 |
|--------------------|-------|----------|
| Average error in % | 1.564 | -6.137   |

### 6.3 Conclusions of the departure validation

This section summarizes the validation results which are given in the previous sections. From this conclusions are formulated. Table 6.7 gives an overview of the validation results.

From table 6.7, it can be seen that AEDT gives an improved method, with respect to BADA 3.8, to model terminal area aircraft fuel consumption. Subsequently, the coefficients, which are determined from extracted PIANO data, shows sufficient fidelity to model departure fuel consumption. The first three errors represent the validation results of aircraft which are already implemented in AEDT. The standard departure, thrust- and aerodynamic coefficients of these aircraft are already proved to be reliable. Hence the validation results of these aircraft give a clear view on the reliability of the new TSFC coefficients. For the

**Table 6.7:** Departure validation summary

| Aircraft   | AEDT         | BADA 3.8      |
|------------|--------------|---------------|
| A319-100   | 0.853%       | -10.572%      |
| A320-200   | 0.207%       | -16.013%      |
| A321-200   | -5.203%      | -14.093%      |
| A330-300   | -3.883%      | -9.817%       |
| A340-300   | 0.163%       | -2.739%       |
| A340-500   | 1.564%       | -6.137%       |
| <b>AAE</b> | <b>1.98%</b> | <b>9.89 %</b> |

A320 family of aircraft the prior method differed from measured values by about 10 to 15%, while the new method differs by 0 to 5%. Note that for this family of aircraft, this modeling improvement is on the order of 100 lb of fuel per departure.

The last three errors represent the validation results for aircraft which are not implemented in AEDT. These aircraft require the validation of TSFC, thrust and aerodynamic coefficients. The previous paragraph discusses the reliability of the TSFC coefficients. There it is stated that the TSFC coefficients show sufficient fidelity which means that the data generation method as well as the data itself are reliable. The thrust coefficients are determined from the same data set. Since this data is reliable, it can indirectly be stated that the thrust coefficients are reliable. Hence, the last three errors give understanding in the accuracy or reliability of the aerodynamic coefficients and of the assumption to use departure profiles of family aircraft. The A330/A340 family shows improvements with the new method during departures, with these aircraft the error is now within 5% of the measured fuel consumption. The current method the extract the aerodynamic coefficient and to use standard departure of family aircraft is sufficiently reliable. However further research on the departure templates and the assumption is recommended.

As can be seen in table 6.7, the Average Absolute Error (AAE) of the AEDT and BADA 3.8 method are approximately 2% and 10%, respectively. The usage of PIANO to determine the departure coefficients decreased the fuel consumption modeling error with 8%. Hence there is definitely an improvement in fuel consumption modeling.

## Chapter 7

# Arrival Operations

In this chapter the arrival coefficients, determined in chapters 4 and 5, are validated. In section 7.1 modeled fuel consumption is compared to the fuel consumption of actual flights, as recorded by the FDR. In order to do this, six actual flights are replicated using AEDT in order to simulate thrust values. Conclusions of the arrival validation can be found in section 7.2.

### 7.1 Validation of arrival TSFC and aerodynamic coefficients

For the validation of the arrival coefficients, the method used for the departure (chapter 6) is not appropriate since arrival aircraft typically do not follow a standard procedure. This is because arrival procedures usually vary from flight to flight due to for instance weather conditions, arrival routes and descent profiles, pilot skills and the amount of air traffic at the particular airport. As a result the fuel consumption in one arrival procedure can be significantly different from that in another arrival procedure. Therefore, the arrival coefficients need to be validated on a case per case basis. In order to do this, the fuel flow was calculated using the  $M$ ,  $h$  and  $F_N$  values from a sample FDR flight in AEDT, and then the calculated fuel flow was compared to the measured fuel flow from the FDR.

For two aircraft, three random flights were selected for modeling. This modeling involves matching the altitudes, airspeeds, flap settings and landing gear settings of the FDR flight from 10,000 ft AGL down to the runway. An intermediate output of this process is the thrust required to balance the forces acting on the aircraft. From these parameters, the fuel consumption is calculated.

Replicating a FDR arrival in AEDT is a very time consuming and rather labor intensive process since it involves matching altitudes and airspeeds. Furthermore, different sets of aerodynamic coefficients require different input settings for the procedural profiles in AEDT. This means that in order to see the difference between two different sets of coefficients, the arrival profile needs to be adapted and fine tuned for each set. This does not ensure a conclusive comparison between the sets since the replication of the arrival procedure is subjective to whoever defines it in AEDT, and would greatly influence the results of the fuel consumption.

Therefore the A319-100 and A321-200 aerodynamic coefficients are calculated using PIANO, using the method as explained in chapter 5, to simulate an arrival in AEDT. Fuel consumption is then modeled by making use of the particular TSFC coefficients. Note that for these



aircraft, the aerodynamic parameters used are now from PIANO and not from Airbus. An example of a flight replication is given in the next subsection. Subsequently, the validation results are stated.

### 7.1.1 Example of replicating an FDR flight in AEDT

As mentioned previously, replicating a flight in AEDT involves matching the altitude and the airspeed of the simulation to the FDR data. This is done by using the procedural profile function in AEDT, which allows the user to create a customized arrival procedure. Determining which values to use for the start altitudes, the start speeds and the descend angles requires a lengthy trial and error process. A first assumption for these values is made by simply looking at FDR output figures, but then the values are further adjusted in an iteration process until the arrival procedures match as closely as possible. An example procedural profile to replicate FDR arrival can be found in table 7.1.

**Table 7.1:** Procedural profile to replicate FDR arrival

| Step # | Type             | Flaps ID | Start Alt. [ft] | Start CAS [kts] | Descend angle [deg] | Track Dist. [ft] | Thrust Type     |
|--------|------------------|----------|-----------------|-----------------|---------------------|------------------|-----------------|
| 1      | D-D <sup>a</sup> | ZERO     | 10,000          | 225             | 2.2                 | -                | -               |
| 2      | Level            | ZERO     | 7655            | 200             | -                   | 22,500           | -               |
| 3      | D-D              | ZERO     | 7655            | 200             | 2.6                 | -                | -               |
| 4      | Descend          | ZERO     | 5429            | 195             | 1.3                 | -                | -               |
| 5      | Level            | ZERO     | 4665            | 195             | -                   | 10,000           | -               |
| 6      | D-D              | ZERO     | 4665            | 190             | 3.5                 | -                | -               |
| 7      | D-D              | 1        | 3267            | 188             | 3.2                 | -                | -               |
| 8      | D-D              | 2_D      | 2429            | 166             | 3.2                 | -                | -               |
| 9      | D-D              | 3_D      | 2218            | 164             | 3.2                 | -                | -               |
| 10     | D-D              | FULL_D   | 2020            | 152             | 3.2                 | -                | -               |
| 11     | Land             | FULL_D   | -               | -               | -                   | 250              | -               |
| 12     | Decelerate       | -        | -               | 113             | -                   | 2300             | RT <sup>b</sup> |
| 13     | Decelerate       | -        | -               | 30              | -                   | 0                | RT              |

<sup>a</sup>D-D: Descend-Decelerate

<sup>b</sup>RT: Reverse Thrust

Figure 7.1 shows the results of the arrival (replication) procedure for an A319-100. The continuous line represents the actual flight as recorded in the FDR, the dotted line shows the output of the AEDT simulation. From figure 7.2(a) it can be seen that the approach profile (altitude vs. ground distance) of the AEDT simulation almost perfectly corresponds with the actual FDR flight. The true airspeed replication does not always match perfectly as this can be seen in figure 7.2(b). In this figure there are two jumps in the FDR true airspeed graph which are not accurately simulated in AEDT.

Using the step inputs of table 7.1 in the simulation, AEDT outputs values for thrust for each time step. These thrust values are then used in equation 4.1 to calculate the TSFC and the fuel flow is determined with equation 6.1. Multiplying the fuel flow with the duration of each time step then gives the modeled fuel consumption. The fuel flow and the consumed fuel for the A319-100 example arrival can be seen in figure 7.2.

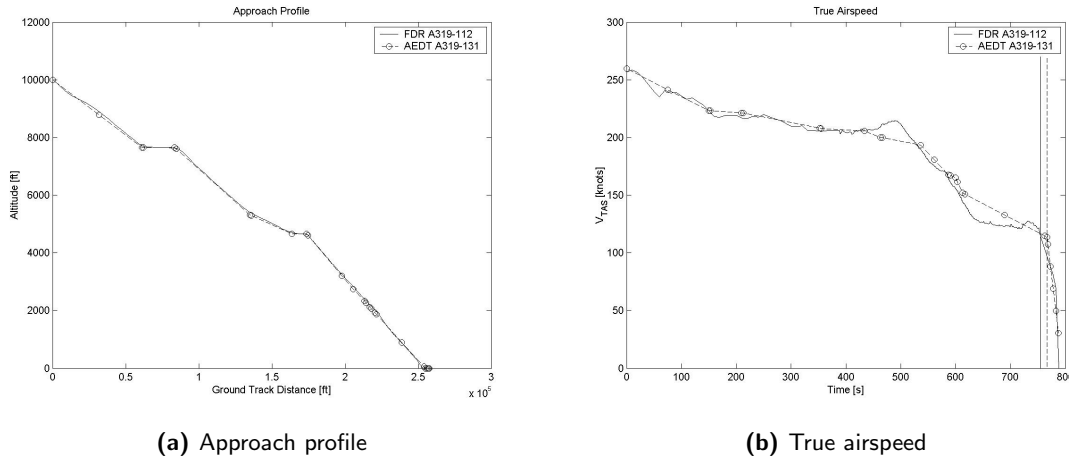


Figure 7.1: Output AEDT simulation of the A319-100

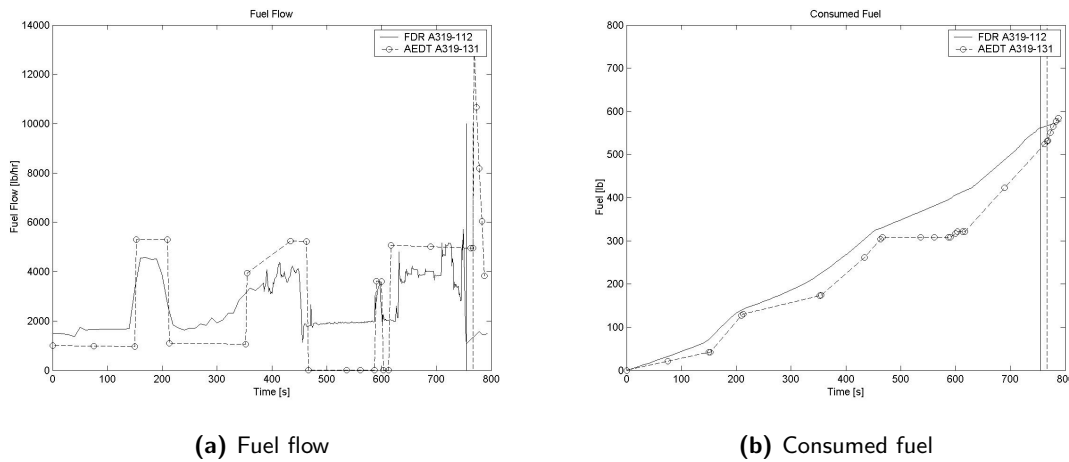


Figure 7.2: Output AEDT simulation of the A319-100

### 7.1.2 Summary of results

The same lengthy procedure has been performed for six random flights from the FDR. Table 7.2 shows the difference between the calculated AEDT consumed fuel and the FDR consumed fuel for these six arrivals. The fuel consumption modeling from BADA 3.8 (previous method) is also shown. The errors are in fact the percentage aberrance between the FDR fuel consumption and the modeled fuel consumption for an arrival from 10,000 ft AGL until the runway.

The validation results in table 7.2 do not correspond with the one of the departure validation. For half of the modeled arrivals, the absolute error of the old BADA 3.8 method is smaller than the one of the new AEDT method. This is likely due to the accuracy of the true airspeed replication. To recall, the TSFC equation of BADA 3.8 depends only on the true airspeed, so possible offsets in true airspeed replication can have a favorable effect on the error. On the other hand, the average absolute error of the modeled arrivals show an improvement in fuel consumption modulation. This error decreased with approximately 4%,

**Table 7.2:** Model comparison results

| Flight            | AEDT error   | BADA error   |
|-------------------|--------------|--------------|
| A319-100 Flight 1 | 4.66%        | 21.93 %      |
| A319-100 Flight 2 | -5.52%       | -1.03%       |
| A319-100 Flight 3 | -1.72%       | 2.79%        |
| A321-200 Flight 1 | 5.26%        | 4.84%        |
| A321-200 Flight 2 | 0.16%        | 19.00%       |
| A321-200 Flight 3 | -12.40%      | 5.66%        |
| <b>AAE</b>        | <b>4.95%</b> | <b>9.21%</b> |

to be more precise from 9% to 5%. Based on the limited number of results, it can partially be stated that the new TSFC and aerodynamic coefficients as well as their determination methods are able to simulate an arrival and model the fuel consumption with sufficient fidelity. More validation results are required to make a more conclusive statement.

## 7.2 Conclusion of the arrival validation

The AEDT method does, for a limited validation set, capture the fuel consumption more closely than BADA 3.8. The average absolute error decreased with 4%. For AEDT this error is determined at approximately 5%, which indicates that the aerodynamic coefficients are sufficiently reliable to simulate an arrival and that the TSFC coefficients are accurate enough to model the fuel consumption.

However, it needs to be mentioned again that the results of the modeled fuel consumption are subjective to many variables. The calculated TSFC coefficients, the calculated aerodynamic coefficients and also the approach profile defined by the user in AEDT, all have a significant influence in the modeled total fuel consumption of any given arrival procedure. Therefore, when results are not conclusive, and vary like they do in table 7.2, it is necessary to perform more simulations of arrival procedures in order to ensure that all coefficient sets - TSFC and aerodynamic coefficients - are conclusive enough to model fuel consumption in AEDT.

## Chapter 8

# Conclusions and Recommendations

This chapter summarizes the general conclusions that are based on the results in the report. Also, some recommendations are given for further improvements and future work on this topic.

### 8.1 Conclusions

The departure coefficients, i.e. TSFC, thrust and aerodynamic coefficients, are validated on the basis of six aircraft by comparing modeled fuel consumption with FDR fuel consumption for departures until 10,000 ft AGL.

For the Airbus A320 family of aircraft, i.e. A319-100, A320-200 and A321-200, the prior BADA 3.8 method differed from measured values of departure fuel consumption by about 10 to 15%. The new AEDT method, with PIANO generated TSFC coefficients, differs by 0 to 5%. Note that for this family of aircraft, this modeling improvement is on the order of 100 lb of fuel per departure. The A320 family of aircraft only required the determination of TSFC coefficients since Airbus has provided the performance data, i.e. thrust and aerodynamic coefficients. This means that the TSFC coefficients show sufficient fidelity to model fuel consumption. It also means that the data sets from which they are determined as well as the data generation/determination method is sufficiently reliable. This indirectly proves that the thrust coefficients are accurate since they are calculated from the same data.

The Airbus A330-200, A340-300 and A340-500 required the determination of the complete coefficient data set (thrust, TSFC and aerodynamic). The validation results of the AEDT method also show improvements during departure. For these aircraft the error is within 5% of the measured fuel consumption, and the average absolute error decreased from 6% (BADA 3.8 method) to 2% (AEDT method). These AEDT errors are relatively low which indicates that the complete data set of each aircraft is reliable to simulate a departure with AEDT software and to model the fuel consumption in the terminal area. However, the aerodynamic coefficients and its determination method show sufficient fidelity, since the previous paragraph already states the reliability of the TSFC and thrust coefficients.

The average absolute error (of all six aircraft) of the AEDT and BADA 3.8 method are approximately 2% and 10%, respectively. The usage of PIANO to determine the departure coefficients decreased the fuel consumption modeling error with 8%. Hence, there is a definite improvement in departure fuel consumption modeling.

The arrival coefficients, TSFC and aerodynamic coefficients, are validated for the Airbus A319-100 and A321-200 by comparing modeled fuel consumption with FDR fuel consumption for an arrival from 10,000 ft AGL until the runway. Modeled fuel consumption is determined by replicating a FDR arrival in AEDT, with PIANO generated coefficients. In total six flights, three for each aircraft, were replicated in AEDT.

The validation results do not correspond with the one of the departure validation. For half of the modeled arrivals, the absolute error of the old BADA 3.8 method is smaller than the one of the new AEDT method. On the other hand, the average absolute error of the validation results shows an improvement in fuel consumption modulation. This error decreased from about 9% (BADA 3.8) to 5%. The 4% improvement indicates that the aerodynamic coefficients are sufficiently reliable to simulate an arrival and that the TSFC coefficients are accurate enough to model the fuel consumption. However, due to the limited number of validation results, it is not possible to make the improvement statement conclusive. This requires more validation results.

The general conclusion of this report is that the new coefficient data set, developed using PIANO, represents an improvement over the prior method of calculating fuel consumption in the terminal area. Moreover it can be stated, on the basis of the validation results, that PIANO is a reliable performance tool for terminal area operations.

## 8.2 Recommendations

The current TSFC and thrust data extraction methods are mainly based on the flight regimes of jet aircraft. These methods are indeed proven to be very reliable for jet aircraft as this can be derived from the validation results of the Airbus A320 family of aircraft. However, the accuracy of this method will likely decrease for propeller aircraft since the flight regimes of these aircraft differ from those of jet aircraft. It is advised to make a second data extraction method which is more specified for propeller aircraft. Validation of this second extraction method is yet a problem because there is currently no propeller FDR data available.

The departure aerodynamic coefficients are determined from a PIANO's departure simulation output. Each aircraft requires a specified departure template which can then be simulated in PIANO.

The Airbus A330-200, A340-300 and A340-500 are the only aircraft which have a more specified departure template. FDR data and departure profiles of family aircraft did allow a well considered specification. This concerns the determination of the altitudes at which thrust settings are changed, flaps are retracted but also on the average airspeed during the intermediate flap angle. Nevertheless, more FDR data from different airports is required to define the best applicable departure template.

All other aircraft, jet as well as propeller aircraft, are subjected to a general departure template since no reliable source was available to specify a particular departure template. Although this general template is based on ICAO procedures, the accuracy of the coefficients is less than when a template is more specified. Future work is required to specify departure templates of other aircraft.

Validation of coefficients is performed by simulating standard departures with the AEDT

software. However, the Airbus A330-200, A340-300 and A340-500 were not implemented in AEDT and so departures are simulated by using standard departure profiles of family aircraft. The validation results of these aircraft show that it is indeed reasonable to assume that departure profiles of family aircraft show similarities. Nevertheless, it is recommended to determine new standard departure profiles for the Airbus A330-200, A340-300 and A340-500.

The drag-over-lift arrival aerodynamic coefficient is determined by using an equation of INM tech manual [12]. The equation itself is derived from SAE-AIR-1845 [16]. Although the equations itself are the same, the parameter explanation of both manuals differ. SAE states that the drag-over-lift coefficient should be determined as it is used during a typical operation and that nominal corrected net thrust should be calculated for the particular approach segment. While INM states that the corrected net thrust is determined at the final altitude of the approach segment (no average) and it does not mention anything on the operation condition of a particular flap setting. The SAE determination method is the appropriate one to use. Unfortunately, the difference is only noticed at the end of the project. It is recommend that the arrival aerodynamic coefficients are determined like the departure aerodynamic coefficients. Develop one complete arrival maneuver, composed of several approach segments which are related to a particular flap setting. This method will likely increase the accuracy of the drag-over-lift coefficients and so improve the arrival fuel consumption modeling even more.

In order to define the exact value of the arrival improvement, more arrivals have to be replicated in AEDT. The current AEDT arrival coefficients do, for the limited validation results, capture the fuel consumption more closely than BADA 3.8, but the small number of data points makes this a less conclusive statement. Replicating a FDR flight in AEDT is currently the only possibility to validate the coefficients. This is, unfortunately, a very time consuming and rather labor intensive process and it can not be automated with WINBATC.

The use of WINBATC relieved the TSFC and thrust data extraction in PIANO. It would be unfeasible to extract all the required data for all aircraft manually. The written WINBATC scripts are user-friendly to make adjustments in input flight regimes blocks, so it can easily be used future extractions. It is recommended to write a WINBATC script for future projects which require a handling that must be repeated intensively.



# Bibliography

- [1] Eurocontrol Experimental Centre. Base of aircraft data (bada) revision 3.8 database.
- [2] Eurocontrol Experimental Centre. User manual for the base of aircraft data (bada) revision 3.8. Technical Report EEC Technical/Scientific Report No. 2010-003, European Organisation for the Safety of Air Navigation (Eurocontrol Experimental Centre), April 2010.
- [3] European Civil Aviation Conference. Report on standard method of computing noise contours around civil airports. In *ECAC.CEAC Doc 29*, volume 2, 2005.
- [4] FAA. Faa aviation environmental models web-site. [http://www.faa.gov/about/office\\_org/headquarters\\_offices/aep/models/](http://www.faa.gov/about/office_org/headquarters_offices/aep/models/).
- [5] P. Hill and C. Petersen. Mechanics and thermodynamics of propulsion. Reading 2nd edition, Addison-Wesley, MA, 1992.
- [6] J. Lee, I. Waitz, and B. Kim et al. *Transportation Research Part D: Transport and Environment*, Vol. 12, Issue 6, pp 381-395, August 2007.
- [7] IHS Global Limited. Jane's all the the world's aircraft. <http://www.janes.com>, November 2010.
- [8] Lissys Limited, Woodhouse Eves, LE 12 8RL, United Kingdom. *Project Interactive Analysis and Optimization (PIANO), version 5.0.0 (Software tool)*, 2010.
- [9] M. Lourdes. In *AIAA/AAF Aircraft Noise and Emissions Reduction Symposium*, Monterey, California, May 23-25, 2005.
- [10] A. Malwitz, B. Kim, G. Fleming, and et al. Technical Report FAA-EE-2005-03, Federal Aviation Administration, Sept 2005.
- [11] The MathWorks Inc., Natick, Massachusetts. *MATLAB version 7.6 (Software tool)*, 2008.
- [12] Office of Environment and Energy. Federal Aviation Administration, inn 7.0 technical manual edition.
- [13] Department of Transportation Federeral Aviation Administration. Type certification data sheets.
- [14] D. Senzig, G. Fleming, and R. Iovinelli. Modeling of terminal-area airplane fuel consumption. *Journal of Aircraft*, Volume 46, Number 4, pp 1089-1093, July-August 2009.



- [15] D. Senzig, G. Fleming, A. Rapoza, and R. Iovinelli. Technical report, DOT Research and Innovative Technology Administration Environmental Measurement and Modeling Division Volpe Center Air Quality Facility, November 2008.
- [16] Aircraft Noise Society of Automotive Engineers, Committee A-21. Procedure of the calculation of airplane noise in the vicinity of airports. Rept. SAE-AIR-1845 No. 1845, Society of Automotive Engineers, Inc, Warrendale, PA, March 1986.
- [17] Statsoft Inc., Tulsa, Oklahoma. *Statistica version 8*, 2001.
- [18] Wilson WindowWare Inc., Seattle, Washington. *WinBatch, the Batch Language for Windows*, 2001.
- [19] T. Yoder. Development of aircraft fuel burn modeling techniques with applications to global emissions modeling and assessment of the benefits of reduced vertical separation minimums. Master's thesis, Dept. of Aeronautics and Astronautics, Massachusetts Institute of Technology, Cambridge, MA, 2007.

# Appendix A

## Thrust Coefficients

Each sets of thrust coefficients is derived for both rated takeoff power settings (THRUST\_TYPE T) and maximum climb power settings (THRUST\_TYPE C).

| ACFT_ID              | THRUST_TYPE | COEFF_E     | COEFF_F      | COEFF_GA    | COEFF_GB     |
|----------------------|-------------|-------------|--------------|-------------|--------------|
| ATR 42-500 (v05)     | T           | 7283.701051 | -1.93774E+01 | 2.65295E-01 | -1.75011E-05 |
| ATR 42-500 (v05)     | C           | 6741.135216 | -1.70124E+01 | 1.05407E-01 | -3.84268E-06 |
| ATR 72-500 (v05)     | T           | 7618.312258 | -2.02923E+01 | 2.75291E-01 | -1.82545E-05 |
| ATR 72-500 (v05)     | C           | 6430.711339 | -1.62375E+01 | 9.85311E-02 | -3.53829E-06 |
| Airbus A318-100 68t  | T           | 23737.08896 | -2.69736E+01 | 2.28734E-01 | -1.34187E-06 |
| Airbus A318-100 68t  | C           | 17740.50728 | -1.78308E+01 | 1.85113E-01 | 3.73514E-06  |
| Airbus A330-200 230t | T           | 64467.65036 | -5.41493E+01 | 9.16582E-01 | -1.09348E-04 |
| Airbus A330-200 230t | C           | 59840.71644 | -5.86675E+01 | 1.09154E+00 | -1.49267E-05 |
| Airbus A340-300 271t | T           | 33803.0056  | -4.08248E+01 | 3.83589E-01 | -1.96512E-05 |
| Airbus A340-300 271t | C           | 28781.28794 | -2.82832E+01 | 5.31134E-01 | -7.24051E-06 |
| Airbus A340-500 380t | T           | 55675.22164 | -6.72397E+01 | 6.31702E-01 | -3.23558E-05 |
| Airbus A340-500 380t | C           | 39153.53918 | -3.84164E+01 | 7.24927E-01 | -9.96858E-06 |
| BAe ATP              | T           | 7060.247835 | -1.87835E+01 | 2.62793E-01 | -1.77938E-05 |
| BAe ATP              | C           | 6237.577661 | -1.58129E+01 | 9.85655E-02 | -3.55860E-06 |
| Canadair CRJ 200ER   | T           | 8588.167929 | -1.08148E+01 | 1.19595E-01 | -1.54851E-06 |
| Canadair CRJ 200ER   | C           | 7221.049876 | -7.93567E+00 | 1.09133E-01 | -2.59514E-07 |
| Canadair CRJ 200LR   | T           | 8588.167929 | -1.08148E+01 | 1.19595E-01 | -1.54851E-06 |
| Canadair CRJ 200LR   | C           | 7226.081374 | -7.95314E+00 | 1.08703E-01 | -2.33720E-07 |
| Embraer 170 AR       | T           | 13927.55542 | -1.68581E+01 | 8.79897E-02 | 9.35012E-07  |
| Embraer 170 AR       | C           | 10879.90246 | -1.16192E+01 | 1.44481E-01 | 2.94821E-07  |
| Embraer 170 LR       | T           | 13927.55542 | -1.68581E+01 | 8.79897E-02 | 9.35012E-07  |
| Embraer 170 LR       | C           | 10875.99352 | -1.16033E+01 | 1.44606E-01 | 2.90247E-07  |
| Embraer 170 STD      | T           | 13935.23964 | -1.68695E+01 | 8.65579E-02 | 1.00499E-06  |
| Embraer 170 STD      | C           | 10875.99352 | -1.16033E+01 | 1.44606E-01 | 2.90247E-07  |
| Embraer 175 AR       | T           | 13927.55542 | -1.68581E+01 | 8.79897E-02 | 9.35012E-07  |
| Embraer 175 AR       | C           | 10875.99352 | -1.16033E+01 | 1.44606E-01 | 2.90247E-07  |
| Embraer 175 LR       | T           | 13930.2857  | -1.68684E+01 | 8.96943E-02 | 6.54740E-07  |
| Embraer 175 LR       | C           | 10875.99352 | -1.16033E+01 | 1.44606E-01 | 2.90247E-07  |
| Embraer 175 STD      | T           | 13927.55542 | -1.68581E+01 | 8.79897E-02 | 9.35012E-07  |
| Embraer 175 STD      | C           | 10875.09958 | -1.16028E+01 | 1.44823E-01 | 2.81566E-07  |
| Embraer 190 AR       | T           | 17300.69436 | -2.09414E+01 | 1.09605E-01 | 1.11926E-06  |
| Embraer 190 AR       | C           | 13777.41015 | -1.46985E+01 | 1.83127E-01 | 3.71838E-07  |
| Embraer 190 LR       | T           | 17300.69436 | -2.09414E+01 | 1.09605E-01 | 1.11926E-06  |
| Embraer 190 LR       | C           | 13776.92792 | -1.47010E+01 | 1.83294E-01 | 3.67207E-07  |
| Embraer 190 STD      | T           | 17300.69436 | -2.09414E+01 | 1.09605E-01 | 1.11926E-06  |
| Embraer 190 STD      | C           | 13777.41015 | -1.46985E+01 | 1.83127E-01 | 3.71838E-07  |
| Embraer 195 AR       | T           | 17300.69436 | -2.09414E+01 | 1.09605E-01 | 1.11926E-06  |

---

| ACFT_ID         | THRUST_TYPE | COEFF_E     | COEFF_F      | COEFF_GA    | COEFF_GB    |
|-----------------|-------------|-------------|--------------|-------------|-------------|
| Embraer 195 AR  | C           | 13777.41015 | -1.46985E+01 | 1.83127E-01 | 3.71838E-07 |
| Embraer 195 LR  | T           | 17300.69436 | -2.09414E+01 | 1.09605E-01 | 1.11926E-06 |
| Embraer 195 LR  | C           | 13775.47192 | -1.46993E+01 | 1.83757E-01 | 3.42833E-07 |
| Embraer 195 STD | T           | 17303.27034 | -2.09584E+01 | 1.08530E-01 | 1.36580E-06 |
| Embraer 195 STD | C           | 13778.33205 | -1.47003E+01 | 1.82921E-01 | 3.87648E-07 |

# Appendix B

## TSFC Coefficients

The MODE column indicates the whether the TSFC coefficients set corresponds to departure (D) or arrival operations (A). The following table shows which coefficients correspond to each mode:

| MODE      | COEFF1   | COEFF2    | COEFF3    | COEFF4    |
|-----------|----------|-----------|-----------|-----------|
| Departure | $K_1$    | $K_2$     | $K_3$     | $K_4$     |
| Arrival   | $\alpha$ | $\beta_1$ | $\beta_2$ | $\beta_3$ |

| ACFT_ID                | MODE | COEFF1         | COEFF2        | COEFF3         | COEFF4        |
|------------------------|------|----------------|---------------|----------------|---------------|
| ATR 42-500 (v05)       | D    | -2.1011266E-01 | 1.4779349E+00 | -6.3100222E-06 | 4.1057291E-05 |
| ATR 42-500 (v05)       | A    | 2.2119400E-01  | 5.2260000E-01 | 1.4669860E+00  | 9.6519630E+00 |
| ATR 72-500 (v05)       | D    | -1.8021008E-01 | 1.4562942E+00 | -5.1148757E-06 | 3.4518197E-05 |
| ATR 72-500 (v05)       | A    | 2.1650300E-01  | 5.2211800E-01 | 1.4436290E+00  | 9.8424670E+00 |
| Airbus A300 600R       | D    | 3.0396560E-01  | 4.6885133E-01 | -7.8787879E-07 | 9.0385066E-07 |
| Airbus A300 600R       | A    | 3.1485000E-01  | 6.4512000E-01 | 9.4600000E-01  | 1.2071700E+01 |
| Airbus A310-300        | D    | 2.7445450E-01  | 4.6527304E-01 | -5.0926324E-07 | 1.5010475E-06 |
| Airbus A310-300        | A    | 3.3559900E-01  | 4.9722100E-01 | 8.3611000E-01  | 9.0496230E+00 |
| Airbus A318-100 68t    | D    | 3.5639898E-01  | 3.2251926E-01 | -1.1918459E-06 | 5.7352056E-06 |
| Airbus A318-100 68t    | A    | 4.5881300E-01  | 2.8016400E-01 | 9.6347100E-01  | 8.8616620E+00 |
| Airbus A319-100 75t    | D    | 3.9268725E-01  | 3.1544822E-01 | -1.1168695E-06 | 3.5586754E-06 |
| Airbus A319-100 75t    | A    | 4.5976200E-01  | 2.7915900E-01 | 9.7984300E-01  | 8.9993980E+00 |
| Airbus A320-200 77t    | D    | 3.9243676E-01  | 3.1848689E-01 | -1.0803689E-06 | 3.7300072E-06 |
| Airbus A320-200 77t    | A    | 4.6499400E-01  | 2.8011300E-01 | 9.7291400E-01  | 8.7271180E+00 |
| Airbus A321-200 89t    | D    | 3.5940183E-01  | 3.0951907E-01 | -1.2881427E-06 | 5.0390054E-06 |
| Airbus A321-200 89t    | A    | 4.4532000E-01  | 2.7426000E-01 | 9.5074000E-01  | 1.0352070E+01 |
| Airbus A330-200 230t   | D    | 2.9478409E-01  | 4.4637813E-01 | -7.1120369E-08 | 7.3509026E-07 |
| Airbus A330-200 230t   | A    | 3.4020400E-01  | 5.0143700E-01 | 8.5217400E-01  | 8.5032930E+00 |
| Airbus A330-300 230t   | D    | 2.9491195E-01  | 4.4624792E-01 | -6.7588899E-08 | 7.3326247E-07 |
| Airbus A330-300 230t   | A    | 3.4020400E-01  | 5.0143700E-01 | 8.5217400E-01  | 8.5032930E+00 |
| Airbus A340-200 275t   | D    | 3.0043657E-01  | 4.3785357E-01 | -3.9238443E-08 | 1.4922564E-06 |
| Airbus A340-200 275t   | A    | 3.0830000E-01  | 6.3330000E-01 | 9.4569000E-01  | 1.2228140E+01 |
| Airbus A340-300 271t   | D    | 3.0184658E-01  | 4.3899489E-01 | -6.0686895E-08 | 1.4698622E-06 |
| Airbus A340-300 271t   | A    | 3.0890000E-01  | 6.3454000E-01 | 9.4752000E-01  | 1.2227880E+01 |
| Airbus A340-500 380t   | D    | 2.2453371E-01  | 4.4769209E-01 | -9.1635651E-07 | 2.7062664E-06 |
| Airbus A340-500 380t   | A    | 2.9634000E-01  | 5.7698000E-01 | 9.1964000E-01  | 1.4518480E+01 |
| Airbus A340-600 380t   | D    | 2.2290601E-01  | 4.4480280E-01 | -8.7802303E-07 | 2.5212259E-06 |
| Airbus A340-600 380t   | A    | 2.9477000E-01  | 5.7439000E-01 | 9.1798000E-01  | 1.4551710E+01 |
| Airbus A380-800 (569t) | D    | 2.4605424E-01  | 4.5426714E-01 | -7.5503855E-07 | 9.4257051E-07 |
| Airbus A380-800 (569t) | A    | 2.7602000E-01  | 5.7335000E-01 | 1.1139700E+00  | 1.4773850E+01 |

| ACFT_ID              | MODE | COEFF1         | COEFF2        | COEFF3         | COEFF4         |
|----------------------|------|----------------|---------------|----------------|----------------|
| BAe 146-200          | D    | 3.5220842E-01  | 6.9325395E-01 | -2.1189183E-06 | 1.2450496E-05  |
| BAe 146-300          | D    | 3.5602863E-01  | 6.8926780E-01 | -2.0667765E-06 | 1.1916581E-05  |
| BAe 146-300          | A    | 4.2927300E-01  | 7.2137300E-01 | 1.6832090E+00  | 9.4383890E+00  |
| BAe ATP              | D    | -2.0597311E-01 | 1.4878678E+00 | -6.0028404E-06 | 4.1177638E-05  |
| BAe ATP              | A    | 2.1755800E-01  | 5.1813800E-01 | 1.4370020E+00  | 9.5526600E+00  |
| Canadair CRJ 200ER   | D    | 3.1082369E-01  | 6.0677167E-01 | -1.8269471E-06 | 8.5103468E-06  |
| Canadair CRJ 200ER   | A    | 3.7729000E-01  | 6.4790000E-01 | 1.7310700E+00  | 1.0254830E+01  |
| Canadair CRJ 200LR   | D    | 3.1340864E-01  | 6.0359303E-01 | -1.7732013E-06 | 8.2217152E-06  |
| Canadair CRJ 200LR   | A    | 3.7729000E-01  | 6.4790000E-01 | 1.7310700E+00  | 1.0254830E+01  |
| Canadair CRJ 900ER   | D    | 2.5220941E-01  | 4.5580937E-01 | 2.7757288E-06  | 1.0843655E-05  |
| Canadair CRJ 900ER   | A    | 3.8900800E-01  | 5.5547800E-01 | 9.8645500E-01  | 8.9233540E+00  |
| Canadair CRJ 900LR   | D    | 2.5241570E-01  | 4.5790511E-01 | 2.7572347E-06  | 1.0922486E-05  |
| Canadair CRJ 900LR   | A    | 3.8911700E-01  | 5.5801800E-01 | 9.7640800E-01  | 8.8111890E+00  |
| Douglas DC 10-10     | D    | 3.9893031E-01  | 3.3469087E-01 | -1.2029592E-06 | 2.3612916E-06  |
| Douglas DC 10-10     | A    | 4.7876100E-01  | 2.8862000E-01 | 9.9239200E-01  | 8.2864540E+00  |
| Douglas DC 10-30     | D    | 4.1446727E-01  | 3.3941821E-01 | -1.1871744E-06 | 1.7284517E-06  |
| Douglas DC 10-30     | A    | 4.8673600E-01  | 2.9451800E-01 | 9.8733800E-01  | 8.1034820E+00  |
| Douglas MD-11F (630) | D    | 2.8273763E-01  | 4.5825853E-01 | -9.2983225E-07 | 1.0915138E-06  |
| Douglas MD-11F (630) | A    | 3.3132800E-01  | 4.8937500E-01 | 8.3425500E-01  | 9.1820400E+00  |
| Douglas MD-81        | D    | 3.5549383E-01  | 4.0974630E-01 | -1.5366194E-06 | 1.3038580E-05  |
| Douglas MD-81        | A    | 5.3921600E-01  | 3.6818300E-01 | 8.9434400E-01  | 6.8721960E+00  |
| Douglas MD-82-88     | D    | 3.5344662E-01  | 4.1104495E-01 | -1.5751335E-06 | 1.3150246E-05  |
| Douglas MD-82-88     | A    | 5.3915100E-01  | 3.6842700E-01 | 8.9841900E-01  | 6.8937740E+00  |
| Douglas MD-87        | D    | 3.6599636E-01  | 3.9928603E-01 | -1.1758627E-06 | 1.2427388E-05  |
| Douglas MD-87        | A    | 5.3915100E-01  | 3.6842700E-01 | 8.9841900E-01  | 6.8937740E+00  |
| Douglas MD-90-50     | D    | 2.9431157E-01  | 4.9302937E-01 | -1.3210747E-06 | 3.7438752E-06  |
| Douglas MD-90-50     | A    | 3.4154200E-01  | 5.6288400E-01 | 5.8758200E-01  | 9.4929870E+00  |
| Embraer 170 AR       | D    | 3.1350466E-01  | 4.3791991E-01 | 3.2308379E-06  | 5.5109115E-06  |
| Embraer 170 AR       | A    | 3.9183500E-01  | 5.6244200E-01 | 9.7725600E-01  | 8.7227790E+00  |
| Embraer 170 LR       | D    | 3.1228702E-01  | 4.3932607E-01 | 3.2193419E-06  | 5.5933412E-06  |
| Embraer 170 LR       | A    | 3.9183500E-01  | 5.6244200E-01 | 9.7725600E-01  | 8.7227790E+00  |
| Embraer 170 STD      | D    | 3.1207912E-01  | 4.3946215E-01 | 3.2116626E-06  | 5.6165601E-06  |
| Embraer 170 STD      | A    | 3.9183500E-01  | 5.6244200E-01 | 9.7725600E-01  | 8.7227790E+00  |
| Embraer 175 AR       | D    | 3.1228702E-01  | 4.3932607E-01 | 3.2193419E-06  | 5.5933412E-06  |
| Embraer 175 AR       | A    | 3.9183500E-01  | 5.6244200E-01 | 9.7725600E-01  | 8.7227790E+00  |
| Embraer 175 LR       | D    | 3.1214426E-01  | 4.3937962E-01 | 3.2151657E-06  | 5.6100765E-06  |
| Embraer 175 LR       | A    | 3.9567000E-01  | 5.7307800E-01 | 1.0018240E+00  | 8.7239180E+00  |
| Embraer 175 STD      | D    | 3.1228655E-01  | 4.3932618E-01 | 3.2190451E-06  | 5.5934724E-06  |
| Embraer 175 STD      | A    | 3.9183500E-01  | 5.6244200E-01 | 9.7725600E-01  | 8.7227790E+00  |
| Embraer 190 AR       | D    | 3.0166524E-01  | 4.4630421E-01 | 2.9806405E-06  | 4.7471898E-06  |
| Embraer 190 AR       | A    | 3.9022500E-01  | 5.6189500E-01 | 9.9267300E-01  | 8.8231800E+00  |
| Embraer 190 LR       | D    | 3.0093830E-01  | 4.4541701E-01 | 3.0143172E-06  | 4.7955043E-06  |
| Embraer 190 LR       | A    | 3.9022500E-01  | 5.6189500E-01 | 9.9267300E-01  | 8.8231800E+00  |
| Embraer 190 STD      | D    | 3.0166524E-01  | 4.4630421E-01 | 2.9806405E-06  | 4.7471898E-06  |
| Embraer 190 STD      | A    | 3.9022500E-01  | 5.6189500E-01 | 9.9267300E-01  | 8.8231800E+00  |
| Embraer 195 AR       | D    | 3.0166524E-01  | 4.4630421E-01 | 2.9806405E-06  | 4.7471898E-06  |
| Embraer 195 AR       | A    | 3.9022500E-01  | 5.6189500E-01 | 9.9267300E-01  | 8.8231800E+00  |
| Embraer 195 LR       | D    | 3.0198242E-01  | 4.4584038E-01 | 2.9848130E-06  | 4.7307804E-06  |
| Embraer 195 LR       | A    | 3.9022500E-01  | 5.6189500E-01 | 9.9267300E-01  | 8.8231800E+00  |
| Embraer 195 STD      | D    | 3.0156777E-01  | 4.4631203E-01 | 2.9898624E-06  | 4.7505774E-06  |
| Embraer 195 STD      | A    | 3.9022500E-01  | 5.6189500E-01 | 9.9267300E-01  | 8.8231800E+00  |
| Embraer EMB-135      | D    | 5.5763592E-01  | 4.6339355E-01 | -2.2124590E-06 | -9.0101761E-06 |
| Embraer EMB-135      | A    | 5.1489700E-01  | 3.9574900E-01 | 1.6401010E+00  | 5.3549080E+00  |
| Embraer EMB-145      | D    | 5.4440868E-01  | 4.5243633E-01 | -2.1602960E-06 | -8.3376102E-06 |
| Embraer EMB-145      | A    | 5.0338200E-01  | 3.8680800E-01 | 1.6297060E+00  | 5.4145160E+00  |
| Fokker F100 basic    | D    | 4.5424297E-01  | 5.2569392E-01 | -1.0979437E-06 | 2.3211073E-06  |
| Fokker F100 basic    | A    | 4.2780200E-01  | 6.9924400E-01 | 8.5559100E-01  | 8.7804330E+00  |

---

| ACFT_ID          | MODE | COEFF1        | COEFF2        | COEFF3         | COEFF4        |
|------------------|------|---------------|---------------|----------------|---------------|
| Fokker F70 basic | D    | 4.4542486E-01 | 5.1679873E-01 | -1.0879072E-06 | 2.5365585E-06 |
| Fokker F70 basic | A    | 4.2074800E-01 | 6.8972600E-01 | 8.7176700E-01  | 9.0459820E+00 |



## Appendix C

# Aerodynamic Coefficients

The aerodynamic coefficients are shown for both departure (OP\_TYPE D) and arrival operations (OP\_TYPE A). If the coefficient is zero, that means that there was no coefficient to be calculated for those (flap) settings. The following table shows which coefficients correspond to each operation type:

| OP_TYPE   | COEFF_R | COEFF_C_D | COEFF_B |
|-----------|---------|-----------|---------|
| Departure | $R$     | $C_f$     | $B_f$   |
| Arrival   | $R_f$   | $D_f$     |         |

| ACFT_ID              | FLAP_ID    | OP_TYPE | COEFF_R  | COEFF_C_D | COEFF_B  |
|----------------------|------------|---------|----------|-----------|----------|
| ATR 42-500 (v05)     | 0 -D       | D       | 0.05528  | 0         | 0        |
| ATR 42-500 (v05)     | 15 -D      | D       | 0.090354 | 0.641977  | 0.02133  |
| ATR 42-500 (v05)     | FULL_D -35 | A       | 0.155948 | 0.560609  | 0        |
| ATR 42-500 (v05)     | 3_D -25    | A       | 0.127454 | 0.592045  | 0        |
| ATR 42-500 (v05)     | 2_D -15    | A       | 0.09896  | 0         | 0        |
| ATR 42-500 (v05)     | 2_U -15    | A       | 0.082984 | 0         | 0        |
| ATR 42-500 (v05)     | ZERO       | A       | 0.058863 | 0         | 0        |
| ATR 72-500 (v05)     | 0 -D       | D       | 0.053077 | 0         | 0        |
| ATR 72-500 (v05)     | 15 -D      | D       | 0.084631 | 0.583694  | 0.017266 |
| ATR 72-500 (v05)     | FULL_D -45 | A       | 0.172124 | 0.511894  | 0        |
| ATR 72-500 (v05)     | 3_D -30    | A       | 0.13636  | 0.540333  | 0        |
| ATR 72-500 (v05)     | 2_D -15    | A       | 0.095293 | 0         | 0        |
| ATR 72-500 (v05)     | 2_U -15    | A       | 0.079388 | 0         | 0        |
| ATR 72-500 (v05)     | ZERO       | A       | 0.056169 | 0         | 0        |
| Airbus A318-100 68t  | 0 -D       | D       | 0.049375 | 0         | 0        |
| Airbus A318-100 68t  | 10 -D      | D       | 0.072714 | 0         | 0        |
| Airbus A318-100 68t  | 15 -D      | D       | 0.085951 | 0.408071  | 0.009591 |
| Airbus A318-100 68t  | FULL_D -40 | A       | 0.15143  | 0.36065   | 0        |
| Airbus A318-100 68t  | 3_D -20    | A       | 0.103297 | 0.393168  | 0        |
| Airbus A318-100 68t  | 2_D -15    | A       | 0.09143  | 0         | 0        |
| Airbus A318-100 68t  | 2_U -15    | A       | 0.077989 | 0         | 0        |
| Airbus A318-100 68t  | ZERO       | A       | 0.056167 | 0         | 0        |
| Airbus A330-200 230t | 0 -D       | D       | 0.041198 | 0         | 0        |
| Airbus A330-200 230t | 8 -D       | D       | 0.065303 | 0         | 0        |
| Airbus A330-200 230t | 14 -D      | D       | 0.079084 | 0.238736  | 0.003394 |
| Airbus A330-200 230t | FULL_D -32 | A       | 0.137381 | 0.21484   | 0        |
| Airbus A330-200 230t | 3_D -22    | A       | 0.109886 | 0.225152  | 0        |
| Airbus A330-200 230t | 2_D -14    | A       | 0.088227 | 0         | 0        |
| Airbus A330-200 230t | 2_U -14    | A       | 0.07377  | 0         | 0        |



| ACFT_ID              | FLAP_ID      | OP_TYPE | COEFF_R  | COEFF_C_D | COEFF_B  |
|----------------------|--------------|---------|----------|-----------|----------|
| Airbus A330-200 230t | ZERO         | A       | 0.05     | 0         | 0        |
| Airbus A340-300 271t | 0 -D         | D       | 0.045224 | 0         | 0        |
| Airbus A340-300 271t | 17 -D        | D       | 0.087066 | 0         | 0        |
| Airbus A340-300 271t | 22 -D        | D       | 0.097662 | 0.226405  | 0.003193 |
| Airbus A340-300 271t | FULL_D -32   | A       | 0.138216 | 0.214883  | 0        |
| Airbus A340-300 271t | 3_D -26      | A       | 0.121738 | 0.221445  | 0        |
| Airbus A340-300 271t | 2_D -22      | A       | 0.110674 | 0         | 0        |
| Airbus A340-300 271t | 2_U -22      | A       | 0.097608 | 0         | 0        |
| Airbus A340-300 271t | ZERO         | A       | 0.051146 | 0         | 0        |
| Airbus A340-500 380t | 0 -D         | D       | 0.047992 | 0         | 0        |
| Airbus A340-500 380t | 17 -D        | D       | 0.08685  | 0         | 0        |
| Airbus A340-500 380t | 22 -D        | D       | 0.101879 | 0.199936  | 0.002338 |
| Airbus A340-500 380t | FULL_D -34   | A       | 0.147279 | 0.195032  | 0        |
| Airbus A340-500 380t | 3_D -29      | A       | 0.133747 | 0.199334  | 0        |
| Airbus A340-500 380t | 2_D -22      | A       | 0.113741 | 0         | 0        |
| Airbus A340-500 380t | 2_U -22      | A       | 0.100489 | 0         | 0        |
| Airbus A340-500 380t | ZERO         | A       | 0.052203 | 0         | 0        |
| Canadair CRJ 200ER   | 0 -D         | D       | 0.059564 | 0         | 0        |
| Canadair CRJ 200ER   | 8 -D         | D       | 0.080331 | 0         | 0        |
| Canadair CRJ 200ER   | 20 -D        | D       | 0.113821 | 0.681923  | 0.029525 |
| Canadair CRJ 200ER   | FULL_D -40   | A       | 0.201884 | 0.650531  | 0        |
| Canadair CRJ 200ER   | 3_D -20      | A       | 0.130189 | 0.733062  | 0        |
| Canadair CRJ 200ER   | 2_D -8       | A       | 0.091915 | 0         | 0        |
| Canadair CRJ 200ER   | 2_U -8       | A       | 0.068158 | 0         | 0        |
| Canadair CRJ 200ER   | ZERO         | A       | 0.056697 | 0         | 0        |
| Canadair CRJ 200LR   | 0 -D         | D       | 0.059917 | 0         | 0        |
| Canadair CRJ 200LR   | 8 -D         | D       | 0.079145 | 0         | 0        |
| Canadair CRJ 200LR   | 20 -D        | D       | 0.113215 | 0.681964  | 0.029654 |
| Canadair CRJ 200LR   | FULL_D -40   | A       | 0.201884 | 0.650531  | 0        |
| Canadair CRJ 200LR   | 3_D -20      | A       | 0.130189 | 0.733062  | 0        |
| Canadair CRJ 200LR   | 2_D -8       | A       | 0.091915 | 0         | 0        |
| Canadair CRJ 200LR   | 2_U -8       | A       | 0.068158 | 0         | 0        |
| Canadair CRJ 200LR   | ZERO         | A       | 0.056697 | 0         | 0        |
| Embraer 170 AR       | 0 -D         | D       | 0.055599 | 0         | 0        |
| Embraer 170 AR       | 5 -D         | D       | 0.065298 | 0         | 0        |
| Embraer 170 AR       | 10 -D        | D       | 0.072584 | 0.555332  | 0.016874 |
| Embraer 170 AR       | FULL_D -34.3 | A       | 0.130086 | 0.486125  | 0        |
| Embraer 170 AR       | 3_D -19.4    | A       | 0.097196 | 0.513568  | 0        |
| Embraer 170 AR       | 2_D -9.5     | A       | 0.078876 | 0         | 0        |
| Embraer 170 AR       | 2_U -9.5     | A       | 0.063968 | 0         | 0        |
| Embraer 170 AR       | ZERO         | A       | 0.077339 | 0         | 0        |
| Embraer 170 LR       | 0 -D         | D       | 0.05635  | 0         | 0        |
| Embraer 170 LR       | 5 -D         | D       | 0.065707 | 0         | 0        |
| Embraer 170 LR       | 10 -D        | D       | 0.072985 | 0.555211  | 0.016932 |
| Embraer 170 LR       | FULL_D -34.3 | A       | 0.130083 | 0.486304  | 0        |
| Embraer 170 LR       | 3_D -19.4    | A       | 0.097199 | 0.513757  | 0        |
| Embraer 170 LR       | 2_D -9.5     | A       | 0.078866 | 0         | 0        |
| Embraer 170 LR       | 2_U -9.5     | A       | 0.063977 | 0         | 0        |
| Embraer 170 LR       | ZERO         | A       | 0.06043  | 0         | 0        |
| Embraer 170 STD      | 0 -D         | D       | 0.058479 | 0         | 0        |
| Embraer 170 STD      | 5 -D         | D       | 0.065591 | 0         | 0        |
| Embraer 170 STD      | 10 -D        | D       | 0.07433  | 0.557369  | 0.017012 |
| Embraer 170 STD      | FULL_D -34.3 | A       | 0.130086 | 0.486312  | 0        |
| Embraer 170 STD      | 3_D -19.4    | A       | 0.097201 | 0.513765  | 0        |
| Embraer 170 STD      | 2_D -9.5     | A       | 0.078867 | 0         | 0        |
| Embraer 170 STD      | 2_U -9.5     | A       | 0.064009 | 0         | 0        |
| Embraer 170 STD      | ZERO         | A       | 0.077359 | 0         | 0        |

| ACFT_ID         | FLAP_ID      | OP_TYPE | COEFF_R  | COEFF_C_D | COEFF_B  |
|-----------------|--------------|---------|----------|-----------|----------|
| Embraer 175 AR  | 0 -D         | D       | 0.055648 | 0         | 0        |
| Embraer 175 AR  | 5 -D         | D       | 0.065411 | 0         | 0        |
| Embraer 175 AR  | 10 -D        | D       | 0.072096 | 0.55643   | 0.016909 |
| Embraer 175 AR  | FULL_D -34.3 | A       | 0.130364 | 0.490022  | 0        |
| Embraer 175 AR  | 3_D -19.4    | A       | 0.097359 | 0.51682   | 0        |
| Embraer 175 AR  | 2_D -9.5     | A       | 0.079039 | 0         | 0        |
| Embraer 175 AR  | 2_U -9.5     | A       | 0.064061 | 0         | 0        |
| Embraer 175 AR  | ZERO         | A       | 0.060586 | 0         | 0        |
| Embraer 175 LR  | 0 -D         | D       | 0.056614 | 0         | 0        |
| Embraer 175 LR  | 5 -D         | D       | 0.066066 | 0         | 0        |
| Embraer 175 LR  | 10 -D        | D       | 0.072796 | 0.557393  | 0.016958 |
| Embraer 175 LR  | FULL_D -34.3 | A       | 0.130083 | 0.486304  | 0        |
| Embraer 175 LR  | 3_D -19.4    | A       | 0.097199 | 0.513757  | 0        |
| Embraer 175 LR  | 2_D -9.5     | A       | 0.078866 | 0         | 0        |
| Embraer 175 LR  | 2_U -9.5     | A       | 0.063977 | 0         | 0        |
| Embraer 175 LR  | ZERO         | A       | 0.06043  | 0         | 0        |
| Embraer 175 STD | 0 -D         | D       | 0.056803 | 0         | 0        |
| Embraer 175 STD | 5 -D         | D       | 0.065815 | 0         | 0        |
| Embraer 175 STD | 10 -D        | D       | 0.073914 | 0.556465  | 0.01701  |
| Embraer 175 STD | FULL_D -34.3 | A       | 0.13036  | 0.490191  | 0        |
| Embraer 175 STD | 3_D -19.4    | A       | 0.097361 | 0.516999  | 0        |
| Embraer 175 STD | 2_D -9.5     | A       | 0.079029 | 0         | 0        |
| Embraer 175 STD | 2_U -9.5     | A       | 0.06407  | 0         | 0        |
| Embraer 175 STD | ZERO         | A       | 0.060575 | 0         | 0        |
| Embraer 190 AR  | 0 -D         | D       | 0.053617 | 0         | 0        |
| Embraer 190 AR  | 7 -D         | D       | 0.069925 | 0         | 0        |
| Embraer 190 AR  | 10 -D        | D       | 0.076302 | 0.506015  | 0.01429  |
| Embraer 190 AR  | FULL_D -36   | A       | 0.149034 | 0.430454  | 0        |
| Embraer 190 AR  | 3_D -20      | A       | 0.108367 | 0.467737  | 0        |
| Embraer 190 AR  | 2_D -10      | A       | 0.084609 | 0         | 0        |
| Embraer 190 AR  | 2_U -10      | A       | 0.068779 | 0         | 0        |
| Embraer 190 AR  | ZERO         | A       | 0.058146 | 0         | 0        |
| Embraer 190 LR  | 0 -D         | D       | 0.052794 | 0         | 0        |
| Embraer 190 LR  | 7 -D         | D       | 0.070207 | 0         | 0        |
| Embraer 190 LR  | 10 -D        | D       | 0.077218 | 0.507498  | 0.014331 |
| Embraer 190 LR  | FULL_D -36   | A       | 0.149022 | 0.431031  | 0        |
| Embraer 190 LR  | 3_D -20      | A       | 0.10836  | 0.468365  | 0        |
| Embraer 190 LR  | 2_D -10      | A       | 0.084608 | 0         | 0        |
| Embraer 190 LR  | 2_U -10      | A       | 0.068781 | 0         | 0        |
| Embraer 190 LR  | ZERO         | A       | 0.058165 | 0         | 0        |
| Embraer 190 STD | 0 -D         | D       | 0.053941 | 0         | 0        |
| Embraer 190 STD | 7 -D         | D       | 0.071481 | 0         | 0        |
| Embraer 190 STD | 10 -D        | D       | 0.07764  | 0.508333  | 0.014422 |
| Embraer 190 STD | FULL_D -36   | A       | 0.148978 | 0.431036  | 0        |
| Embraer 190 STD | 3_D -20      | A       | 0.108338 | 0.46837   | 0        |
| Embraer 190 STD | 2_D -10      | A       | 0.084609 | 0         | 0        |
| Embraer 190 STD | 2_U -10      | A       | 0.068805 | 0         | 0        |
| Embraer 190 STD | ZERO         | A       | 0.058188 | 0         | 0        |
| Embraer 195 AR  | 0 -D         | D       | 0.053973 | 0         | 0        |
| Embraer 195 AR  | 7 -D         | D       | 0.069927 | 0         | 0        |
| Embraer 195 AR  | 10 -D        | D       | 0.076122 | 0.51542   | 0.015004 |
| Embraer 195 AR  | FULL_D -36   | A       | 0.149    | 0.428819  | 0        |
| Embraer 195 AR  | 3_D -20      | A       | 0.108436 | 0.465103  | 0        |
| Embraer 195 AR  | 2_D -10      | A       | 0.084738 | 0         | 0        |
| Embraer 195 AR  | 2_U -10      | A       | 0.068939 | 0         | 0        |
| Embraer 195 AR  | ZERO         | A       | 0.05843  | 0         | 0        |
| Embraer 195 LR  | 0 -D         | D       | 0.053062 | 0         | 0        |

| ACFT_ID          | FLAP_ID    | OP_TYPE | COEFF_R  | COEFF_C_D | COEFF_B  |
|------------------|------------|---------|----------|-----------|----------|
| Embraer 195 LR   | 7 -D       | D       | 0.070105 | 0         | 0        |
| Embraer 195 LR   | 10 -D      | D       | 0.076862 | 0.516999  | 0.015037 |
| Embraer 195 LR   | FULL_D -36 | A       | 0.148987 | 0.429361  | 0        |
| Embraer 195 LR   | 3_D -20    | A       | 0.108429 | 0.465692  | 0        |
| Embraer 195 LR   | 2_D -10    | A       | 0.084737 | 0         | 0        |
| Embraer 195 LR   | 2_U -10    | A       | 0.068941 | 0         | 0        |
| Embraer 195 LR   | ZERO       | A       | 0.058449 | 0         | 0        |
| Embraer 195 STD  | 0 -D       | D       | 0.054114 | 0         | 0        |
| Embraer 195 STD  | 7 -D       | D       | 0.070855 | 0         | 0        |
| Embraer 195 STD  | 10 -D      | D       | 0.077461 | 0.518341  | 0.015098 |
| Embraer 195 STD  | FULL_D -36 | A       | 0.148945 | 0.429366  | 0        |
| Embraer 195 STD  | 3_D -20    | A       | 0.108409 | 0.465697  | 0        |
| Embraer 195 STD  | 2_D -10    | A       | 0.084737 | 0         | 0        |
| Embraer 195 STD  | 2_U -10    | A       | 0.068963 | 0         | 0        |
| Embraer 195 STD  | ZERO       | A       | 0.058471 | 0         | 0        |
| Fokker F70 basic | 0 -D       | D       | 0.055331 | 0         | 0        |
| Fokker F70 basic | 8 -D       | D       | 0.07741  | 0.523533  | 0.015275 |

## **Appendix D**

# **AEDT Output Example**

AIRPLANE OPERATIONS

0 acft\_id = A320-211  
eng\_type = J (Jet, Turboprop, Piston)  
stat\_thrust = 25000 (Pounds)  
thrust\_type = L (P=Percent, L=Pounds, X=Other)  
owner\_cat = C (Commercial, GenAviation, Military)  
op\_type = D (A=appr, D=dep, T=touch&go, F=ci rcuit, V=overflight, R=runup)  
numb\_ops = 1.0000, 0.0000, 0.0000 (day, eve, ngt)  
frst\_a\_nois = 0  
numb\_a\_nois = 7  
frst\_p\_nois = 7  
numb\_p\_nois = 7  
model\_type = I (Inm, Noi semap)  
spect\_nums = 202, 103, 0 (approach, depart, afterburner)  
flt\_path = D-09-1-0-1 CAQA-1  
numb\_segs = 29

| seg | start-x | start-y | start-z | uni t-x | uni t-y | uni t-z | length  | speed | d. spd | thrust  | d. thr  | op | flaps  | bank | duration |
|-----|---------|---------|---------|---------|---------|---------|---------|-------|--------|---------|---------|----|--------|------|----------|
| 0   | 0.0     | 0.0     | 0.0     | 1.0000  | 0.0000  | 0.0000  | 73.9    | 0.0   | 19.9   | 24056.4 | -472.5  | D  | -NONE- | 0.0  | 4.4      |
| 1   | 73.9    | 0.0     | 0.0     | 1.0000  | 0.0000  | 0.0000  | 221.7   | 19.9  | 19.9   | 23583.9 | -472.5  | D  | -NONE- | 0.0  | 4.4      |
| 2   | 295.6   | 0.0     | 0.0     | 1.0000  | 0.0000  | 0.0000  | 369.5   | 39.8  | 19.9   | 23111.4 | -472.5  | D  | -NONE- | 0.0  | 4.4      |
| 3   | 665.0   | 0.0     | 0.0     | 1.0000  | 0.0000  | 0.0000  | 517.2   | 59.7  | 19.9   | 22638.8 | -472.5  | D  | -NONE- | 0.0  | 4.4      |
| 4   | 1182.3  | 0.0     | 0.0     | 1.0000  | 0.0000  | 0.0000  | 665.0   | 79.6  | 19.9   | 22166.3 | -472.5  | D  | -NONE- | 0.0  | 4.4      |
| 5   | 1847.3  | 0.0     | 0.0     | 1.0000  | 0.0000  | 0.0000  | 812.8   | 99.4  | 19.9   | 21693.8 | -472.5  | D  | -NONE- | 0.0  | 4.4      |
| 6   | 2660.1  | 0.0     | 0.0     | 1.0000  | 0.0000  | 0.0000  | 960.6   | 119.3 | 19.9   | 21221.3 | -472.5  | D  | -NONE- | 0.0  | 4.4      |
| 7   | 3620.6  | 0.0     | 0.0     | 0.9752  | 0.0000  | 0.2213  | 210.1   | 139.2 | 0.1    | 20748.7 | 12.8    | D  | -NONE- | 0.0  | 0.9      |
| 8   | 3825.5  | 0.0     | 46.5    | 0.9752  | 0.0000  | 0.2213  | 250.8   | 139.3 | 0.1    | 20761.6 | 15.3    | D  | -NONE- | 0.0  | 1.1      |
| 9   | 4070.1  | 0.0     | 102.0   | 0.9752  | 0.0000  | 0.2213  | 298.2   | 139.5 | 0.1    | 20776.8 | 18.2    | D  | -NONE- | 0.0  | 1.3      |
| 10  | 4360.9  | 0.0     | 168.0   | 0.9752  | 0.0000  | 0.2213  | 376.2   | 139.6 | 0.2    | 20795.0 | 22.9    | D  | -NONE- | 0.0  | 1.6      |
| 11  | 4727.7  | 0.0     | 251.3   | 0.9752  | 0.0000  | 0.2213  | 504.9   | 139.8 | 0.2    | 20817.9 | 30.7    | D  | -NONE- | 0.0  | 2.1      |
| 12  | 5220.1  | 0.0     | 363.0   | 0.9752  | 0.0000  | 0.2213  | 748.9   | 140.0 | 0.4    | 20848.5 | 45.4    | D  | -NONE- | 0.0  | 3.2      |
| 13  | 5950.5  | 0.0     | 528.8   | 0.9752  | 0.0000  | 0.2213  | 1331.8  | 140.4 | 0.7    | 20893.9 | 80.4    | D  | -NONE- | 0.0  | 5.6      |
| 14  | 7249.3  | 0.0     | 823.5   | 0.9752  | 0.0000  | 0.2213  | 3056.7  | 141.1 | 1.5    | 20974.2 | 183.1   | D  | -NONE- | 0.0  | 12.8     |
| 15  | 10230.1 | 0.0     | 1500.0  | 0.9883  | 0.0000  | 0.1523  | 1011.8  | 142.5 | 0.4    | 21157.3 | -4372.3 | D  | -NONE- | 0.0  | 4.2      |
| 16  | 11230.1 | 0.0     | 1654.1  | 0.9883  | 0.0000  | 0.1523  | 8838.1  | 142.9 | 3.1    | 16785.1 | 308.1   | D  | -NONE- | 0.0  | 36.3     |
| 17  | 19965.1 | 0.0     | 3000.0  | 0.9989  | 0.0000  | 0.0477  | 2078.6  | 146.0 | 15.2   | 17093.1 | -38.2   | D  | -NONE- | 0.0  | 8.0      |
| 18  | 22041.4 | 0.0     | 3099.1  | 0.9989  | 0.0000  | 0.0477  | 2284.7  | 161.2 | 15.2   | 17055.0 | -38.2   | D  | -NONE- | 0.0  | 8.0      |
| 19  | 24323.4 | 0.0     | 3208.0  | 0.9989  | 0.0000  | 0.0477  | 2490.8  | 176.4 | 15.2   | 17016.8 | -38.1   | D  | -NONE- | 0.0  | 8.5      |
| 20  | 26811.4 | 0.0     | 3326.8  | 0.9989  | 0.0000  | 0.0466  | 2854.8  | 191.7 | 16.6   | 16978.7 | -37.9   | D  | -NONE- | 0.0  | 8.5      |
| 21  | 29663.1 | 0.0     | 3459.9  | 0.9987  | 0.0000  | 0.0502  | 2646.4  | 208.3 | 15.0   | 16940.8 | -29.7   | D  | -NONE- | 0.0  | 7.3      |
| 22  | 32306.2 | 0.0     | 3592.9  | 0.9987  | 0.0000  | 0.0502  | 2830.7  | 223.3 | 15.0   | 16911.1 | -29.7   | D  | -NONE- | 0.0  | 7.3      |
| 23  | 35133.3 | 0.0     | 3735.1  | 0.9988  | 0.0000  | 0.0498  | 2495.9  | 238.3 | 12.3   | 16881.3 | -20.3   | D  | -NONE- | 0.0  | 6.0      |
| 24  | 37626.0 | 0.0     | 3859.4  | 0.9988  | 0.0000  | 0.0498  | 2621.3  | 250.6 | 12.3   | 16861.0 | -20.3   | D  | -NONE- | 0.0  | 6.0      |
| 25  | 40244.1 | 0.0     | 3989.9  | 0.9902  | 0.0000  | 0.1396  | 10819.2 | 262.9 | 6.3    | 16840.6 | 332.6   | D  | -NONE- | 0.0  | 24.1     |
| 26  | 50957.4 | 0.0     | 5500.0  | 0.9913  | 0.0000  | 0.1313  | 15228.7 | 269.2 | 8.7    | 17173.2 | 601.5   | D  | -NONE- | 0.0  | 33.0     |
| 27  | 66054.3 | 0.0     | 7500.0  | 0.9926  | 0.0000  | 0.1212  | 20629.0 | 278.0 | 11.5   | 17634.7 | 609.3   | D  | -NONE- | 0.0  | 43.1     |
| 28  | 86531.2 | 0.0     | 10000.0 | 0.9926  | 0.0000  | 0.1212  | 1.0     | 289.4 | 0.0    | 18244.0 | 0.0     | D  | -NONE- | 0.0  | 0.0      |